

Current and emerging trends in polymeric 3D printed microfluidic devices

Gustavo Gonzalez ^{a,b}, Ignazio Roppolo ^{a,c}, Annalisa Chiappone ^{a,c}, Fabrizio Pirri ^{a,b,c}

^a *Department of Applied Science and Technology, Polytechnic of Turin, C.so Duca Degli Abruzzi 24, Turin, 10129, Italy*

^b *Center for Sustainable Futures @ Polito, Italian Institute of Technology, Via Livorno 60, Turin, 10144, Italy*

^c *Polito BIOMed Lab, Polytechnic of Turin, C.so Duca Degli Abruzzi 24, Turin, 10129, Italy*

* Correspondence: XXXXXXXXXXXXXXXX@polito.it

Abstract

3D printing technology has been considered a valid alternative for producing microfluidic devices during the last two decades. 3D printing introduces new strategies to obtain high precision microfluidic parts without complex tools and machines that can make the production of microfluidic devices cheaper, faster, and easier than conventional microfluidic fabrications methods such as soft-lithography. Among the main 3D techniques used for this purpose, fused filament manufacturing (FFF), inkjet 3D printing (i3Dp) and vat polymerization (VP) are of the greatest interest since they are well-established techniques in the field and are cost-affordable both in equipment and material. However, for polymeric 3D printing to establish itself as a real production technique for microfluidics chips, there are still some barriers in terms of technology and materials to overtake. For example, the level of resolution and precision of 3D printed microfluidic parts still does not reach the level of conventional techniques (only in some specific cases and through strategies that are not very easy to implement), and, from a materialistic point of view, few materials present the desired characteristics (e.g., biocompatibility, optical transparency, and mechanical properties) for specific sectors such as medicine, analytical chemistry, and pharmaceuticals. This review intends to evaluate and analyze the current state of 3D printing techniques and their materials for the manufacture of microfluidic chips. The article will show and discuss the latest innovations, materials, and applications of such 3D printed microstructures. This review's main focus is to provide an overview of recent and future developments in 3D printing and materials in the branch of microfluidics fabrications. By selecting the right materials and the design freedom afforded by 3D printing, unique structures with interesting properties might be produced.

Keywords: 3D printing, polymer, microfluidic, additive manufacturing, lab on a chip

1. Introduction

Over the last decades, microfluidic devices have been used for different applications, especially chemistry and biology, introducing new analytical and laboratory procedures [1–3]. Many of these microdevices have been applied to study cancer cells' growth and metastasis, analyzing the interaction of such carcinogenic entities with other cells, to model illnesses and testing or screening new drugs [4–7]. The interest in microfluidics lies mainly in the possibility of performing laboratory analyses on a micrometer scale, allowing savings in sample consumption and reducing the overall costs compared to conventional laboratory procedures [8–10]. Researchers have used microfluidics for a myriad of applications in chemistry, biology, and medicine owing to a series of benefits: high spatial resolution and sensitivity, low volume consumption, fast processing, and easiness of integration with electronic elements. Microfluidic chips are assembled with a series of sub-millimeter channels, specifically designed to achieve the desired features, e.g., mixing, pumping, or sorting the liquid passing through them [3,11–13]. Connecting such microfluidics with a few electronic elements, the devices (known as lab-on-a-chip) might be used in different biochemical applications for controlling/monitoring the behavior of specific analytical solutions, useful for rapid DNA sequencing, electrophoretic separation, wearable sensors, organ-on-chip development and disease diagnosis in point-of-care settings with a high level of precision [14–17]. Currently, there are different methods to produce microfluidic devices, e.g., micromachining, soft-lithography, (hot)-embossing, injection molding, and laser ablation, among the principals [18–20]. Most of these methods require controlled environments or cleanroom facilities to work properly and might not be compatible with mass production. Other shortcomings are complex control systems, non-standard user interfaces, fabrication speed, and material modeling cost. Hence, microfluidic devices' potential growth is somehow confined to research laboratories due to the tedious and expensive fabrications methods, limiting their diffusion [21]. Therefore, more and more efforts are currently devoted to producing microfluidic devices through easier and cheaper approaches that might aid the success of microfluidics beyond laboratories.

Researchers have been using 3D printing (3DP) technologies (for a couple of years now) to produce fluidic devices with satisfactory results and aided by recent technological advancements in the field. Such technology is one of the most thriving technologies nowadays that can potentially make a great contribution in the microfluidic field. 3D printing can overcome microfluidics barriers associated with mass production by enabling lower-cost and simplest fabrication of such devices in fewer steps [22–29]. 3DP enables the on-demand production of parts from different materials that can be used in numerous industrial and research applications [30–33]. The principle behind this technology is the fabrication of three-dimensional objects from a digital model design through a single machine. The digital model (commonly in Computer-Aided Design or CAD format) is cross-sectioned by dedicated computer software. The objects are then fabricated by the selective and successive addition of material until the part is completed. 3DP offers different benefits for part production; for instance, complex-shaped structures can be easier to obtain compared to conventional processes, parts can be obtained in a matter of minutes or hours from a digital file without requiring tools or molds, and can lead to saving in materials utilization and consumption, overall production costs, and energy, among others [34–36]. Today, many different 3D printing technologies have been developed. They can be classified based on the type of material used, how materials are joined, and the working principle; each brings unique characteristics [37]. The different 3DP techniques have been extensively evaluated in multiple literature reviews, based on the type of printable material used, application areas, benefits, and drawbacks [30,37–43].

Polymeric 3D printing offers multiple advantages for the medical and biomedical fields, e.g., relatively fast printing times, cost-affordable materials and equipment, accessibility, and high printing resolutions [44–51]. These features make polymeric 3DP a promising method for numerous biomedical applications, e.g., prototyping organ models, producing *in-vitro* platforms for cell culturing, scaffold structures for tissue engineering, on-demand fabrication of medical implants and prostheses, and multiple medical situations where it is required a fast production of customized parts [44,46,51–57]. Indeed, during the recent pandemic crisis, polymeric 3D printing demonstrated that it could be used in hospitals for the fast production of plastic valves and connectors for addressing the shortage of respiratory tools during the coronavirus disease (COVID-19) caused by the novel coronavirus (Sars-CoV-2) [58–61]. For microfluidic fabrications, not all 3D printing techniques are appropriate. Microfluidic devices should gather some essential criteria for their correct operation, such as flexibility, biocompatibility, precise design and geometry, and optical transparency, which only a few polymeric 3D printing techniques can meet. Different studies have reported the 3D printing of polymeric microfluidic devices for various *in-vitro* studies, such as bioreactors for real-time biological analysis or analytical systems [25–29]. Most of these studies are mainly focused on using methods such as (see Fig. 1) fused filament fabrication (FFF), inkjet-based 3DP, e.g., Polyjet and Multijet, and vat polymerization methods, e.g., stereolithography (SL) and digital light processing (DLP). This review intends to present the state-of-the-art about the latest material development, 3D printed part features such as optical transparency, printing resolution and biocompatibility, and the technological 3D printing trends considering the aforementioned methods to compete with conventional procedures for microfluidic chips fabrications. We examine the most relevant applications of 3D-printed microfluidic devices, highlighting the main barrier found in the literature to adopt this technology to microfluidics scenarios related to personalized medicine systems and point-of-care devices.

2. 3D printing of polymeric microfluidic devices

Numerous studies have reported the use of polymeric 3DP for microfluidic devices fabrication (see Fig. 1), showing the vast number of publications and citations per year over the last two decades using the keywords “microfluidic” and the name of a single 3D printing method [25–29,62–64]. Fig. 1 **Error. L'origine riferimento non è stata trovata.** also considers the term 3D printing to include other not well-known terms in the area of microfluidic fabrication. The acceptance of polymeric 3DP for microfluidic fabrication is evident. The number of publications in 2021 has increased more than ten times compared to the year 2010, and almost four times compared to the year 2015 (a trend that increases by analyzing the number of citations per year, with $\times 20$ and $\times 6$ in 2020 compared to 2010 and 2015, respectively). Interestingly, while the diagram of 3D printing and Microfluidic (both N° publications and citations per year) increases, the graph of Polydimethylsiloxane (PDMS) and Microfluidic start to decrease from 2010 forward. Probably this trend is not only due to the appearance of 3D printing for microfluidic chips fabrication, as other microfabrication technologies and materials have appeared in recent years; however, such a trend shows that the scientific community has been searching for, for about a decade, an alternative to conventional microfabrication methods. Most of these published works about 3D printing and microfluidic are focused on using mainly fused filament fabrication (FFF), Polyjet/Multijet, and vat polymerization techniques, i.e., stereolithography and digital light processing, since they are well-established techniques that present a good compromise between printing resolution/accuracy, printing speed and material availability [45,65,66]. Each of the 3D printing methods offers different

characteristics that can be beneficial according to the microfluidic system and its application, as summarized in Table 1. The most requested characteristics of 3D printed polymeric microfluidics are biocompatibility, optical transparency, and microchannels' reliability. The following section will present an overview of current trends and strategies to fabricate microfluidic chips by polymeric 3D printing.

1.1. Fused Filament Fabrication methods for microfluidic devices fabrication

Fused deposition modeling (FDM), also known as fused filament fabrication (FFF), is probably the most representative 3D printing method [45,67,68]. As schematized in Fig. 2.a, in these 3D printing techniques, the material (filament) is extruded through a nozzle by thermal effect. Other 3D printing techniques follow a similar extrusion-processing principle, although they use a screw, piston, or pneumatic force (pressurized air or gas) to induce the material deposition [38]. In general, extrusion-based 3D printing consists of a motorized system with a three-axis motion that allows material deposition selectively. The material is first deposited at the preferred position in the *XY* plane to achieve the first layer. Then a second layer is deposited onto the prior one by either the building platform moving down or the extrusion nozzle moving up; the process is repeated until the final part is obtained [69].

The fused deposition modeling (FDM) technique was invented by Scott Crump in 1989 [40,70], and after the patent expired in 2009, people started to fabricate FDM printers independently without compensating *Stratasys* (the company that branded the FDM technique), decreasing equipment and materials costs. *Stratasys* is still proprietary of the FDM term, and now, these methods are known as Fused Filament Fabrication (FFF) [71]. The success of FFF lies in their larger palette of available printable materials (see Table 1), their relatively lower cost and their more user-friendly systems and software. FFF works by heating thermoplastic filaments (linear molecules) above its glass transition temperature through a heated nozzle. The softened material is first deposited onto the building platform (following the specifications from the computer) and then cooled down below its glass transition temperature [72]. The resolution and performance of FFF methods depend on various parameters, such as temperature, the viscosity of the extruded filament, layer height, layer density, shear force, nozzle diameter printing velocity and type of material. Hence, it is essential to balance these printing parameters to reach reliable printing resolutions and accuracy and avoid defects during the 3D printing step. Today, FFF-based 3D printers can be found with a printing resolution of 10 μm , a building size as large as 200 x 200 x 400 mm^3 , and a building speed as high as 500 mm/s [73,74]. The most common issue between FFF users is the inadequate adhesion between layers, leading to objects with poor mechanical properties. Such phenomenon occurs when some printing variables, such as the temperature of the processing, the temperature of the building platform (creating thermal shrinkage), and physicochemical properties of the material (e.g., heat transfer), are not well defined [69]. Another common shortcoming of FFF methods is the lack of mechanical strength of the molten thermoplastic (it might not support itself during slow cooling) [38]. Indeed, some FFF machines use a secondary filament to support the object temporarily. This support material can be later removed by immersion in water or other types of solvents. Other drawbacks of FFF-based 3D printing are the vertical anisotropy, step structured surface (meaning low superficial resolution), layer adhesion between layers, porosities or air trapped between layers and nozzle clogging [72].

In FFF-3D printing methods, more than one nozzle can be used in the same printing process. Each nozzle can be loaded with different materials, enabling the manufacture of multi-material

structures that display different properties and features in a single 3D printed object [75]. The printable filaments can also be loaded with fillers, fibers, dyes, and other additives (e.g., carbon black, glass fiber, carbon fiber and metallic powders), looking to impart specific characteristics. Various thermoplastic polymers with different features can be used in FFF-based 3D printing. The most common thermoplastics materials are polystyrene, polycarbonate (PC), acrylonitrile-butadiene-styrene copolymers (ABS), polymethylmethacrylate (PMMA), polylactic acid (PLA), polyetheretherketone (PEEK), poly- ϵ -caprolactone (PCL), and Polyamide or Nylon; few of them with biocompatible properties [69,71,76–79]. Fig. 4 shows the chemical structure of commonly used thermoplastics for FFF-3D printing. An alternative method to FFF printing is Direct Ink Writing or DIW (not discussed in this review), in which a viscoelastic material is printed (Fig. 2.b-d) [80,81]. This technique can use air pressure, a piston, or a screw to extrude the material onto the building platform. In this case, the solidification of the material can be achieved by thermal effect, photopolymerization, chemical crosslinking, rapid phase transition, and fast solvent evaporation rate, and instead of printable filaments, the DIW technique uses viscoelastic materials (or inks) with suitable rheological properties. The rheological properties of the printable ink should guarantee continuity of extrusion and be self-consistent to ensure the correct piece formation during the layer-by-layer step [82]. Typical DIW inks are made of polymers mixed with suitable organic solvents or water to adjust the viscosity of the printable material. Besides, inks of high-molecular-weight oligomers or pastes with high inorganic material content can be used [83]. DIW can process a great variety of materials since many available polymers exhibit good rheological properties. In addition, DIW can be set with multiple dispensers and composite inks, allowing multi-material and functional structures fabrication. The most used materials for DIW are silicone elastomers, polyurethane, fluorinated polymers, cellulose and gelatin-based (see Fig. 4), hydrogels polymer-based colloids, nanocomposite (e.g., graphene oxide, carbon nanotubes, silver nanowires or MXenes) and even biological material (in this case, the printing techniques are better referred to as bioprinting) [84–90]. One of the main disadvantages of DIW is the low printing velocity and resolution. In optimized conditions, the DIW can reach a printing resolution in the order of micrometers, but on the other hand, the printing time increases [86]. The highest DIW printing speed reported to date is 100 mm/s, far below the speed of others printing techniques for polymers [40].

FFF methods offer microfluidic chip fabrication benefits, such as cost-affordable materials and equipment, high printing speed, and standardized and user-friendly apparatus. Moreover, a vast range of commercially available and biocompatible filaments can be processed for microfluidic chips fabrications. Through FFF methods, interesting fluidic devices have been created with satisfactory results in transparency, resolution, and biocompatibility. For example, Bressan et al. developed 3D-printed microfluidic chips based on polylactic acid (PLA) to synthesize silver and gold nanoparticles [91,92]. By optimizing the printing parameter, the chips were fabricated with channels as small as 260 μm x 260 μm employed to well-control the fluid flow behavior for obtaining particles with the desired features. These particles were then used for biological applications such as crystal violet (CV) through SERS analysis or to improve the electrocatalytic capability of carbon paste electrode (CPE) for the electrochemical determination of gallic acid (GA) and thiocyanate ions. During FFF printing processes, the wall surfaces of the printed parts can be rough due to the deposition of melted filaments. Therefore, channels with a well-established sidewall dimension are quite challenging to produce with such a 3D printing technique.

Nevertheless, the surface roughness of the microfluidic channel surface might be used as an advantage in some cases. For example, Li et al. demonstrated how the extruded filament orientation

could enhance fluidic behavior control [93]. They developed various microfluidic chips (channels of 500 μm x 500 μm) with different printing orientations of the filament (0°, 30°, 60°, and 90°) respecting the fluid flow direction to examine the fluid mixing performance (Fig. 3.a). These chips were produced with good optical transparency using a commercial filament, Crystal Clear acrylonitrile-butadiene-styrene (ABS) from *3D Systems*. Li and coworkers showed that in microfluidic chips, where the extruded filament was oriented at 60° to the flow direction, the mixing of fluids in laminar flow was achieved without any complex channel geometry or other passive mixers.

Moreover, the authors demonstrated that chips' mixing performance could be adjusted by changing the filament orientation at 0° and 90°. The researchers performed simple colorimetric assays to measure the content of iron in environmental water samples, where is desired a mixing property. The fabrication of truly microfluidic devices (<100 μm) is still challenging using FFF-3D printing. The typically requested microchannel dimensions are much smaller than most of the extruded filaments and nozzles available today. Moreover, another shortcoming of FFF-3D printing is that only a few thermoplastic filaments might be used to produce optically transparent structures, which is one of the most requested characteristics of microfluidic devices for allowing the correct real-time visualization of the fluids. Some interesting strategies have been followed in this sense. For example, Kotz and coworkers produced transparent chips using commercially available polymethylmethacrylate (PMMA) filament, one of the most used materials for microfluidic chip fabrication [94]. With PMMA filaments (from *Material4print*), the authors created chips with a minimum channel width of about 300 μm x 300 μm . The chips' bottom transparency (the region of interest for proteins patterning) was significantly improved by directly printing onto PMMA sheets (not created by FFF 3d printing). These chips were used for mixing dyed water. The chip's surface was then selectively photopatterned with fluorescently labeled biotin (F5B), showing the easy biofunctionalization of 3D printed closed PMMA chips (Fig. 3.b).

Transparent microfluidic chips were also obtained from Nelson et al. using a commercial thermoplastic polyurethane filament (SainSmart Clear flexible TPU) [95]. They developed microfluidic chips with optical transparency (up to 85 % of transmission), chemical solvent stability, high-pressure resistance, and flexibility (see Fig. 3.c). The printed chips' biocompatibility was demonstrated by culturing mouse inner medullary collecting duct cells (mIMCD3). The researchers produced microfluidic chips with channel features as small as 50 μm x 50 μm (the smallest one by FFF to date) in less than 25 minutes. Other researchers developed transparent and sealed microfluidic chips with PLA as an alternative to conventional polydimethylsiloxane material (PDMS), acting as an electronic tongue (e-tongue). These flexible and interdigitated microfluidic chips were capable of distinguishing tastes below the human threshold. The chips were built within less than one hour, using a homemade 3D printer [96]. In addition to PLA, other types of cost-affordable materials can also be used. As reported in 2018 by Romanov and coworkers, 3D printed microfluidic chips with a channel dimension of about 400 μm were produced with either polylactic acid (PLA) or polyethylene terephthalate glycol (PETg) through two different types of commercially available low-cost FDM-3D printers: Prusa i3 (\$ 600) and LulzBot (\$ 2500) [97]. Such devices presented high-pressure, heat resistance, and glass-like layer characteristics, features that were useful for DNA melting analysis and facilitated the optical visualization of fluids in droplet generation and tracking and identifying DNA. Direct ink writing (DIW) methods have also been used for fabrication microstructures or microfluidic devices. Ching et al. introduced a method for fabricating microfluidic devices by directly depositing the extruded filament material onto a flat substrate using a commercial desktop DIW-3D printer [98]. The material used was a commercial

silicone elastomer (Silicone sealant, Wet Area Speedseal®) patterned onto a sheet of polymethylmethacrylate (PMMA). Once the machine sketched the microchannel features, a second PMMA was used to close the device; then, a laser created the inlets and outlets elements. By intercalating multiple PMMA sheets between each printed silicone microstructure, the authors produced 3D networks of microchannels. Through such DIW method, the researchers could select the substrate (i.e., PMMA) with the required characteristics such as optical transparency and biocompatibility.

Moreover, due to the use of elastomeric materials, they were able to willfully deform the microchannel to control the channel dimension, reaching features as small as near 32 μm (in width) and 20 μm (in height). Through this approach, the authors pointed out three key beneficial points for the manufacturing of microfluidic chips: (1) the possibility of tuning channel dimensions, (2) the possibility of incorporating diverse types of substrates, according to the looked-for characteristic, and (3) the possibility of integrating fluid-handling and functional components such as valve and pumps in the same 3D printing process. Although Ching et al. proposed an interesting way for producing optically transparent microfluidic devices, their method requires certain manual labor to thread the PMMA sheets during 3D printing. On the other side, this method does not require removing supporting material from the microchannels, which could be a great advantage when handling fragile or delicate microfluidic systems. Athanasiadis et al. developed a DIW-based strategy to produce filaments with an internal microfluidic channel [99]. They used the 3D printer (3D discovery bioprinter, Regen HU) to first deposit a filament made of silicone elastomer (polydimethylsiloxane, SE1700 from Dow Corning) and then modify the just deposited filament with the same printing nozzle, used as a “pencil,” to remove part of the material. The authors set the correct printing parameters (i.e., pneumatic pressure, nozzle diameter, nozzle height, and extrusion speed) to perform the post-extrusion modification and create groove-shaped filaments. Programming the stylus nozzle position above the substrate, the groove depth increase making collapse the groove walls, closing it and producing the channel. The width of the groove depends on the external diameter of the printing nozzle, which in the case of the authors was 430 μm . Even though such a strategy allowed the creation of fibers with microfluid channels, the channel dimension depended on the external diameter of the nozzle. Hu et al. described an easy way to produce PDMS-based microfluidic chips using a 3D printed sacrificial microstructure [100]. The researchers used a 3D-plotter (EnvisionTEC) to pattern the material on a PDMS substrate in a petri dish, creating fugitive or sacrificial microstructures for PDMS casting. The material was the water-soluble Pluronic F-127 ink that, once is plotted on the substrate surface, the microstructure was encapsulated with PDMS by casting. By this strategy, microdevices with channel widths varying from 300 to 570 μm were obtained by setting the right printing parameters. The Pluronic F-127 material contained inside the channels was removed, after the PDMS curing, by constantly flushing cold water and ethanol. Such a hybrid manufacturing approach allowed the authors to produce flexible, transparent, and low-cost microfluidic devices used to acetylate various amines through microwave irradiation, obtaining acetamides in shorter reaction times and good yields than conventional chemical methods.

1.2. Inkjet-based 3D printing method (i3Dp)

Inkjet-based 3D printing, i.e., Polyjet and MultiJet, is a method that employs photocurable resins deposited selectively on a platform drop-by-drop, as schematized in Fig. 2.e [101]. After the deposition of the first layer, a UV lamp, located inside the machine chamber, rapidly cures it. The platform stage is lowered, and the next film is built, repeating the process until obtaining the final

structure. During the i3Dp, a blade can be used to smooth the surface of the just printed layer to guarantee a clean and uniform layer before the light-curing phase.

Polyjet 3D printing technique was invented in the latest '90s by Object Ltd (now Stratasys), being nowadays one of the most commercially available 3DP methods. While in 1996, 3D Systems presented their material jetting method commercialized as MultiJet printing [102,103]. A common configuration of these printing techniques consists of various jetting heads, a three-axis motion platform, and the UV-curing device. In most of the Inkjet-based 3D printing methods, the jetting of material can be achieved by two modalities: continuous inkjet (CIJ) and drop-on-demand (DOD) [104,105]. In the CIJ-based methods, the photopolymer is continuously jetted through the nozzle by pressure action, generating a stream of droplets according to the Rayleigh-Plateau instability phenomenon of the liquid column, as described by others works [106,107]. In the DOD-based methods, the pressure pulse generates the droplets, and when this pulse exceeds the threshold at the nozzle, the droplets are ejected. Commonly, the velocity of droplets generation with CIJ-based 3D printing methods is higher than DOD-based ones with >10 m/s and 5–8 m/s, respectively [106]. The printing resolution of the inkjet-based technique is limited to hundreds of micrometers, depending on factors such as droplet diameter, the impact of the droplets onto the platform, the contact angle between the droplet and the substrate [102,106]. During a typical i3D printing condition, the printer heads spray two different materials: the building and support/sacrificial materials (used to maintain the just deposited and still liquid building material) [104,108]. In Polyjet, this sacrificial material combines acrylate monomers and other elements such as polyethylene and propylene that can be removed after the printing step by high-pressure waterjet or solvent dissolution. In MultiJet, the sacrificial material is a wax composition that is melted in a dedicated post-printing process. Both building and sacrificial material should present two crucial requirements for i3Dp use: (i) Appropriate fluid properties to guarantee droplets' correct formation and precise deposition (low-viscosity materials are preferred) and (ii) high photopolymerization (curing) rate to polymerize the deposited material fast, avoiding losing the structure shape [40].

In general, i3Dp formulations are made of a mix of monomers and oligomers, photoinitiators, dyes and other additives. Monomers and oligomers are reactive polymers with functional groups (unsaturated functional groups or C=C) necessary to create the polymeric network. The chemical structures of the most common monomers and oligomers used are depicted in Fig. 4. The backbone of these reagents defines the polymerized part's final physical and mechanical properties (together with the appropriate adhesion between cured layers). Photoinitiators are compounds that absorb part of the incident light, generating reactive species or radicals through chemical transformations. These species interact with monomers and oligomers, enabling the photopolymerization mechanism [109,110]. Table 2 shows the most typical photoinitiators used for 3D printable photopolymers preparation. Dyes or pigments are organic or organometallic molecules used to control the light's penetration during 3D printing (*Z-axis*) to enhance the printing resolution (*X-Y plane*) [111]. Other additives can be combined with printable ink, such as reactive diluents used to adjust the material's viscosity or enhance the solubility of other components such as photoinitiators or dyes [112,113]. Nano-fillers such as silica or clay fillers can also be combined with the printable ink (according to the nozzle diameter and final viscosity of the ink) to enhance the specific characteristic of the final parts, such as the mechanical properties [114].

For microfluidic chips fabrication, photopolymer-based i3Dp is preferred over other material jetting techniques such as thermal-curing-based since they combine the benefits of lithographic

methods (e.g., high spatial resolution, high feature definition and good surface quality) and high build speed, material versatilities and large build volume from material jetting techniques [115]. Using Polyjet or Mulyjet-based printing methods, the printed microchips' surface features could be significantly enhanced compared to FFF-3D printing (although the prices are typically higher than FFF methods). Moreover, with these i3Dp methods, the printing time speed and the microfluidic chips' accuracy can be superior in all axes to the extrusion-based techniques [116]. Lee et al. reported microfluidic chips by PolyJet with a nominal X - Y plane and z dimensions of $500\ \mu\text{m}$ and $100\ \mu\text{m}$, respectively, with an average deviation (between the printed part and the CAD design) of $25.2\ \mu\text{m}$ and with smoother features (surface roughness of $0.47\ \mu\text{m}$) compared to $67.8\ \mu\text{m}$ of average deviation and $42.97\ \mu\text{m}$ of surface roughness of FFF-3D printed parts (

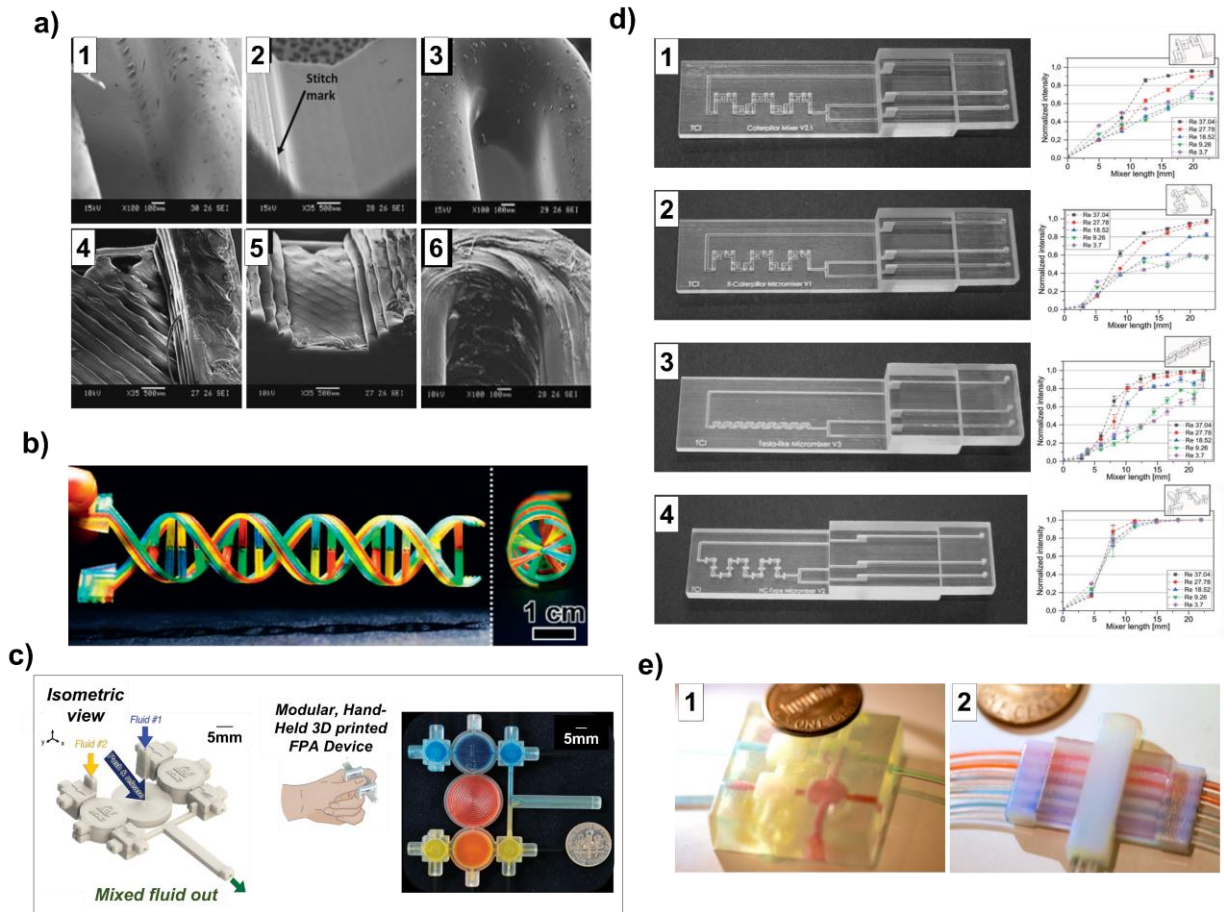


Fig. 5.a) [117]. These microfluidic chips, made from commercial material (FullCure, *Stratasys*), presented high cell viability toward C2C12 cells as a function of an appropriate post-printing sterilization step. Sochol et al. developed advanced components used as fluidic capacitors, diodes, and transistors to construct integrated fluidic circuits (IFC) [118]. The components were fabricated

using a commercial material, Visijet M3 Crystal from 3D Systems (see

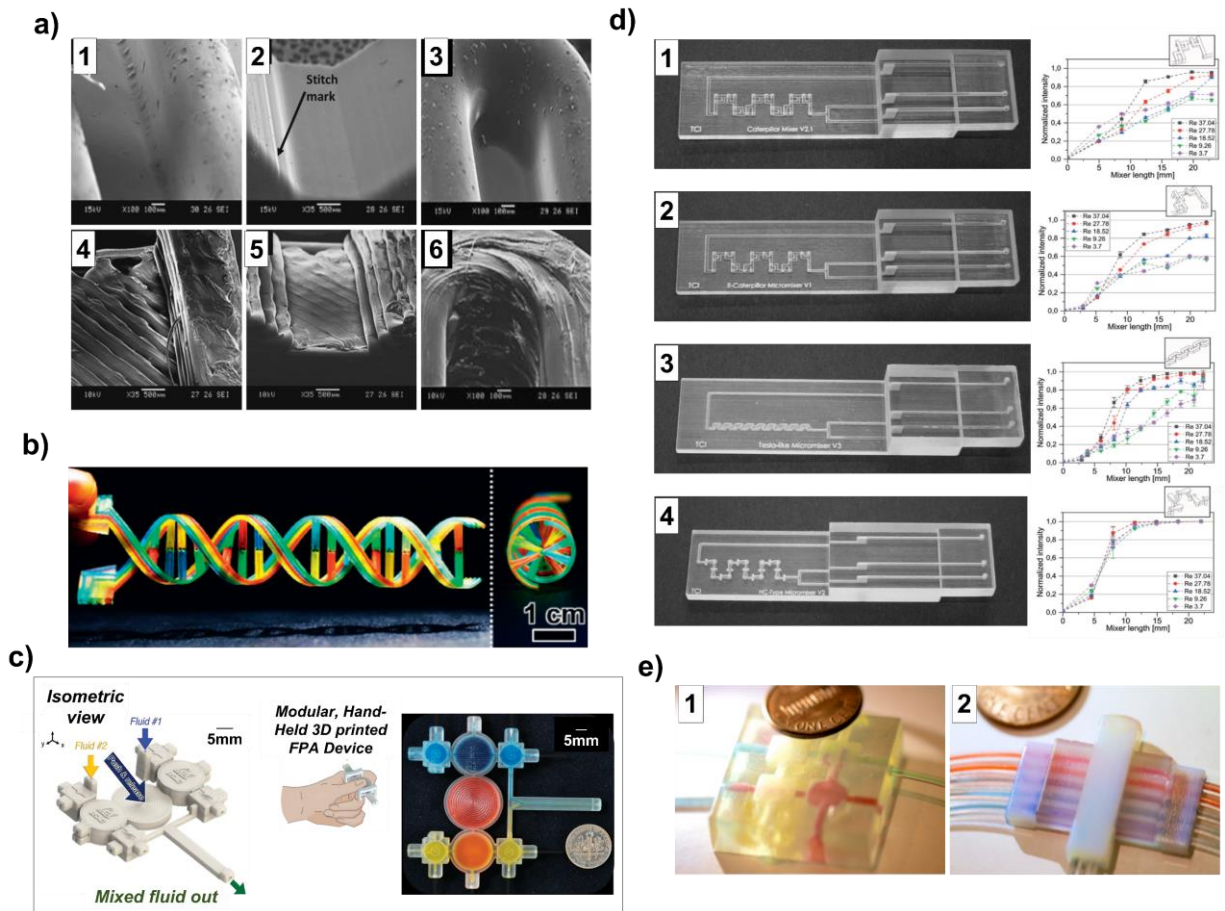


Fig. 5.b), presenting limited biocompatibility. Indeed, the investigators evidenced that further works are required using more biocompatible material for Multijet printing, such as MED610, or performing the appropriate post-processing steps to provide higher biocompatibility to the chips. The authors produced reliable and sophisticated chips in which the functionalities could be customized by modifying the geometric parameters. Sweet and coworkers' work produced a series of finger-powered actuator (FPA) prototypes using Visijet material through PolyJet 3D printing [119]. The pulsatile fluid motion capability of the fabricated devices was used as modular models

for microfluidic actuation and mixing purposes in an integrated fluidic platform; see

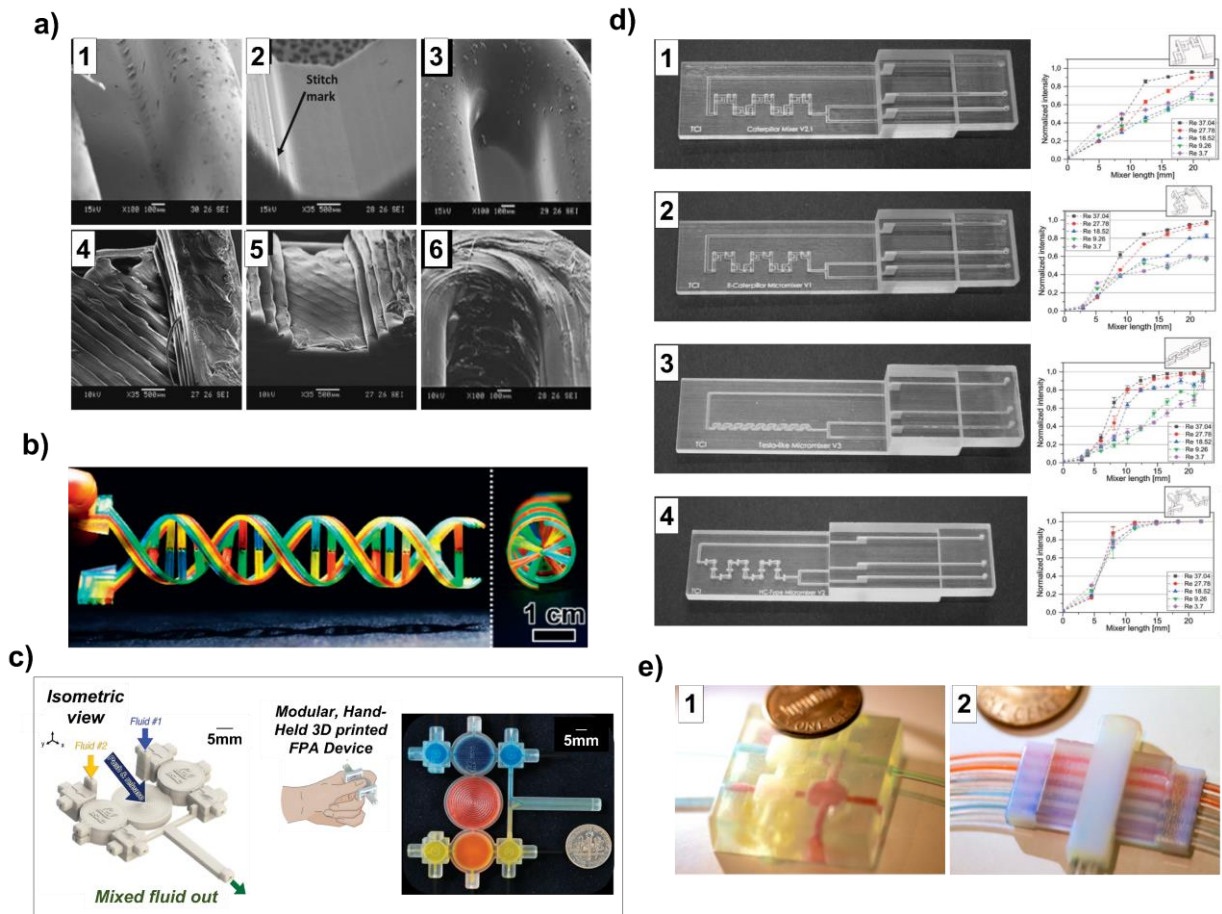


Fig. 5.c. A further advantage of inkjet-based 3D printing is that it allows the fabrication of multiple microfluidic chips contemporaneously with high precision and accuracy. Walczak et al. presented the manufacturing of a series of microfluidic chips (up to 170 chips) during a single 3D printing process. The chips with diameter dimensions of $400\ \mu\text{m}$ and with semi-transparent features were used for capillary gel electrophoresis. After optimizing the printing parameters in terms of printing orientation, fluorescence detection of DNA was possible [120].

In terms of optical transparency, highly transparent chips with intricate microchannels can also be produced using PolyJet for fluid mixing and optical analysis. The fluid profile in most microfluidic systems is in a laminar flow; therefore, mixing different fluids efficiently and rapidly in this regime is a fundamental aspect of microfluidic chips for biological and chemical applications [3,11,12]. Enders et al. produced different micro-passive mixers through PolyJet methods with great optical features and sophisticated channel paths to study and compare the mixing

performances between each configuration (

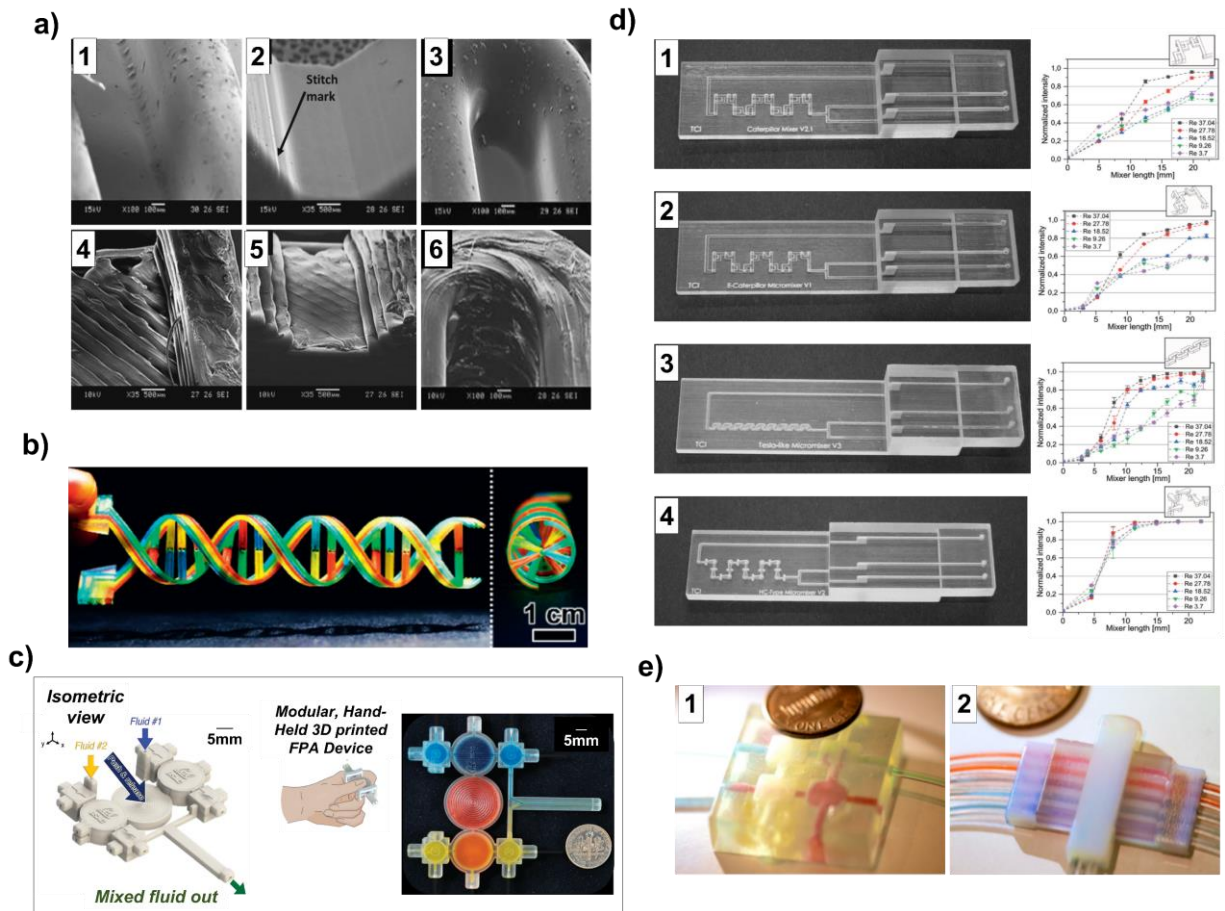


Fig. 5.d) [121]. The designs of the most diffused mixer types, e.g., Caterpillar, enhanced Caterpillar, Tesla-like, and HC mixers, were produced using an acrylate-based material (VisiJet M2R-CL, 3D System). After a series of experimental and simulation comparison tests, they observed that Tesla-like and especially HC chips were the most suitable for the rapid and efficient mixing of biological fluids such as CHO-K1 (Chinese hamster ovary) cells.

The resolution of the i3Dp is higher than extrusion-based methods; however, it is still challenging to obtain sub-100 μm channels since this technique requires using a support material to avoid filling the built microchannel during printing. The removal of the support material after printing implies complex post-printing treatments [22,29,49]. This setback could become even trickier when the microfluidic channel configuration increases in complexity and geometry. In this context, Castiaux and collaborators proposed an interesting strategy: instead of using conventional support material, the researchers stopped the printing process at a certain point to incorporate either a thin polycarbonate membrane or a liquid (composed of glycerol/isopropanol 65:35 v:v) as a physical barrier that can support the additional printed layers [122]. Both techniques demonstrated to be useful for creating complex-shaped microfluidic chips with channels dimensions as small as $15 \times 250 \mu\text{m}$, dimensions difficult to achieve by using conventional support material. However, the results obtained appear difficult to reproduce since the $250 \mu\text{m} \times 15 \mu\text{m}$ channel was initially intended to be $125 \mu\text{m} \times 54 \mu\text{m}$ according to their CAD design. Besides, it must be considered that stopping the printing procedure for placing extra material manually inevitably introduces additional labor in the process. One advantage of the i3Dp is its multi-material versatility by spraying various materials with different characteristics, e.g., mechanical or optical

properties, during the same printing process [38,123]. Taking advantage of this characteristic, S. Keating et al. reported the 3D printing of multi-material valves using both rigid (VeroWhitePlus, RGD835, Stratasys) and flexible (TangoPlus, FLX930, Stratasys) materials. They compared the multi-material valves with single material valves observing that the former present a more robust capability to deformation, enabling better and precise control of fluids, leading to automated production of microfluidic devices (

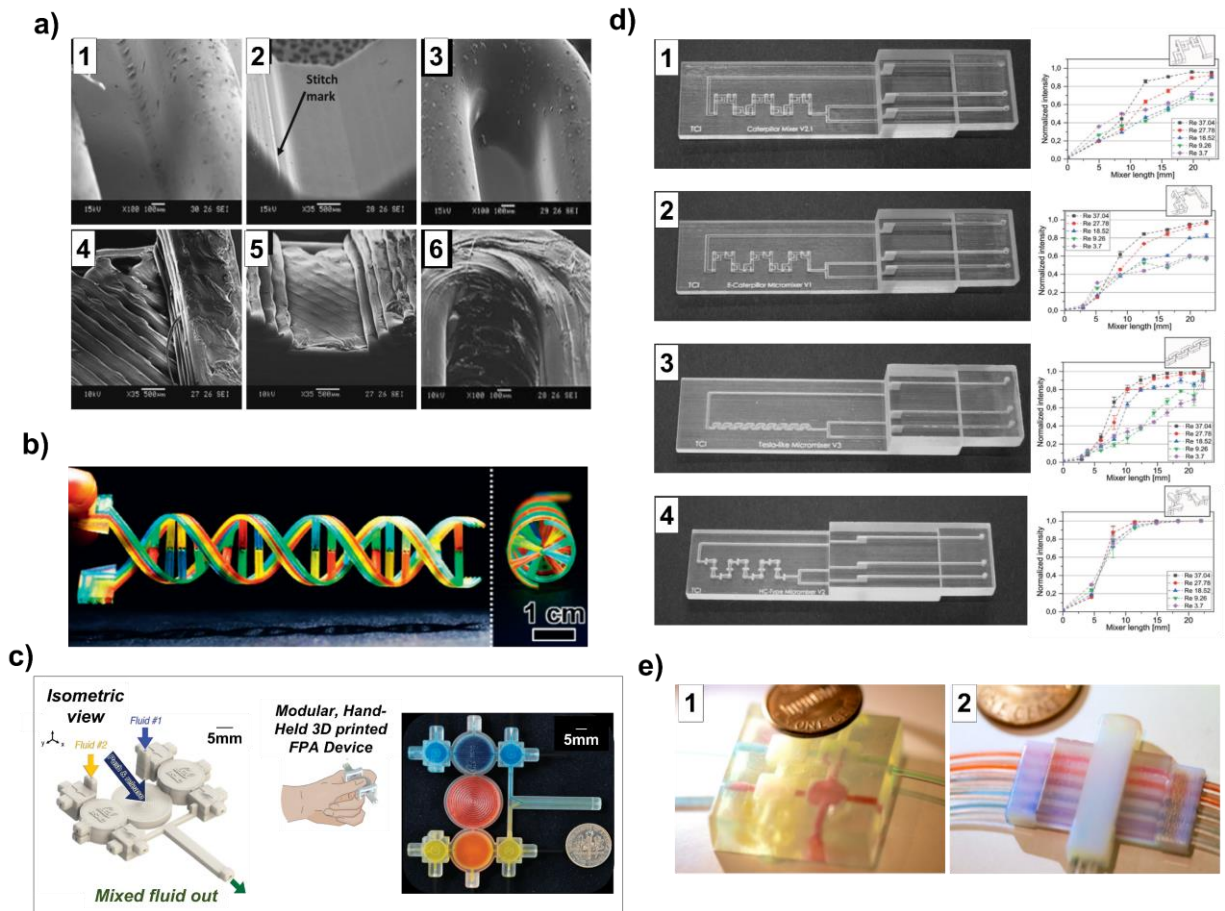


Fig. 5.e) [124]. Keating and coworkers reported that such multipurpose fluidic chips with channels $800\ \mu\text{m} \times 800\ \mu\text{m}$ and programmable valves might be used for various advanced biological applications such as DNA assembly and analysis, continuous sampling sensing and soft robotics.

Hence, the i3Dp techniques can be used for microfluidic chip fabrication with remarkable results, even if this technique requires a considerable post-printing process to clean the microchannels without damaging the microdevices correctly. Other aspects to consider are that i3Dp presents a relatively high initial cost in equipment and consumables. Besides, the window of available materials for i3Dp is limited since they are restrained by the range of viscosity and high curing rate other liquid properties (e.g., ink surface tension) requirements. Moreover, the printable materials are "regulated" formulations, developed only by the owners and therefore difficult to modify or adjust. Finally, more in-depth studies about the biocompatibility of the printable inks are still missing [44,115].

1.3. Vat polymerization method

Vat polymerization (VP) 3D printing is another photopolymerization-based technique that involves using a vat containing a liquid photopolymer [125]. This technique presents valuable

features for microfluidic chips fabrication, e.g., high printing resolution and accuracy, faster printing times, and more flexibility in material tailoring and development than other polymeric 3D printing techniques (see **Errore. L'origine riferimento non è stata trovata.**) [66,125–129]. The VP-3D printing technique was introduced in the early 80s when the stereolithography (SL) method was developed by Hideo Kodama and Charles Hull works [130,131]. In the following years, various SL-based methods were developed, e.g., Digital Light Processing (DLP) [45,132], Micro-Stereolithography 3D printing (μ SL) [133], Continuous Liquid Interface Production (CLIP) [134,135], Two-Photon Polymerization (2PP) [136], and Computed Axial Lithography (CAL) [137]. The stereolithography (SL) method is based on the selective polymerization of photopolymers by using a laser beam focused on the liquid photopolymer, as represented in Fig. 2.f. The polymer is formed by moving the laser over the resin surface (usually using a galvanometric head to control the laser) to create the first layer [138]. This polymerized layer remains attached to the building platform that is lowered according to the layer slicing step. The subsequent layers are 'printed' following the same procedure until the complete fabrication of the object. The printed parts are subjected to post-curing processes to reach the highest chemical conversions possible [54]. SL machines can be configured either top-down (Fig. 2.f) or bottom-up approaches [127]. In the top-down configuration, the light comes from above, and the platform is submerged in the liquid as the part is created. While in the bottom-up, the laser beam hits the resin from the bottom of the vat through a transparent window, and the object remains attached to the platform that rises according to the formation of each layer. Generally, the bottom-up approach is preferred over the top-down since it is not dependent on the vat depth, and it requires less printable material (since it is not necessary to fill the entire vat to print).

With SL-3DP, printing features below 10 μ m can be achieved [139]. At the beginning of the 90s, a derived SL technology was created, the micro-stereolithography 3D printing (MSL or μ SL) with a laser spot of about 5 μ m [133]. Through μ SL-3D printing, structures with sub-1 μ m as a minimum feature size can be achieved [140]. Another SL-based is the Digital Light Processing 3D printing (DLP®). The DLP-based 3D printers are built by deformable mirror device (DMD) chips produced by Texas Instruments (see Fig. 2.g) [141,142]. In these configurations, each micromirror on the DMD represents one pixel in the digital image, which can drive to printing resolutions of 3–5 μ m in the *X-Y* plane according to the optical setup [143]. In the DLP-3D printing configurations, the parts are produced by projecting an entire cross-section of the object (plane-by-plane approach) rather than drawing it by a laser (line-by-line) as the case for SL methods. The photopolymerization of an entire cross-section of the object can significantly reduce printing times compared to SL techniques. Currently, commercial DLP-based printers present printing resolutions as small as 40 x 40 μ m [132]. A variation of DLP-3D printing is the CLIP method that stands for Continuous Liquid Interface Production. CLIP-3D printing allows the continuous fabrication of objects by creating a thin interfacial layer of oxygen through an oxygen-permeable window. This thin oxygen layer (a dead zone) inhibits the free-radical polymerization only in the interface between the polymer film and the transparent window. Therefore, the just-built film does not adhere to the vat bottom; and the printing speed increases considerably up to hundreds of millimeters per hour. With the CLIP approach, large-scale and complex-shaped structures can be produced, maintaining high resolution [134,135]. Other light-based 3D printing methods have been developed in recent years, such as two-photon polymerization (2PP) or Computed Axial Lithography (CAL). The 2PP method (not discussed in this review) is quite similar to stereolithography (SL) in that a laser scan a photopolymer [143]. The main peculiarity of the 2PP process is that the photoinitiator molecule absorbs two photons simultaneously to start the free-radical polymerization, leading to

dimensions in the scale of the nanometer [136,144]. Some of the common drawbacks of 2PP are the limited dimensions of fabrication (no more than 1 mm height) and the lower printing velocity, which is about 0.5-1 mm/s, compared to some SL techniques (200-300 mm/s) [145]. Besides, 2PP requires expensive equipment to set the optical arrangement [146]. Computed Axial Lithography (CAL) is a volumetric configuration developed as an alternative to the layer-by-layer 3D printing approach [137]. CAL methods are based on computed tomography (CT) scans to generate a hologram within a controlled photopolymer volume, as shown in Fig. 2.h [147]. This hologram is created by the simultaneous projection of multiple 2D images while the vat container is rotating. The 2D images propagate through the liquid resin from different angles, resulting in a three-dimensional hologram with enough energy to photocuring, at once, a volume of photopolymer [148]. A fundamental parameter of CAL techniques is the rotation velocity that might directly influence the printing features when the rotary system is not in sync with the projected images. Another parameter of CAL is finding and adjusting the resins' viscosity since it must be high enough to avoid the relative shift between the 3D printed model and the rest of the liquid resin. CAL techniques' advantages are related to great production speed and surface definition, and these techniques can polymerize high viscosity resins (up to approximately 90 000 cP) that are difficult to achieve with other techniques such as DLP or SL [149].

In all these SL-derived 3DP techniques, the printing part enters into contact with the liquid during the printing process. Hence, one crucial point is that the polymerized object is insoluble in the liquid resin, i.e., the cured structure remains dimensionally and mechanically invariable when contacting the liquid resin. Such a condition is achieved by using cross-linkable photopolymers and supplying the system with sufficient light energy to reach the material's gel point (the point where the liquid system starts to show more solid-like mechanical features, becoming insoluble) [125]. As for inks used in i3Dp, photopolymer for VP-3D printing combines, typically, three main chemical components: monomers and oligomers, photoinitiators, and additives. These photopolymers are mainly based on free-radically polymerizable resins, more frequently (meth)acrylate functionalities characterized by unsaturated C=C double bonds [150]. Such reactive groups are employed since they present high reactivity upon light irradiation, well-established mechanisms of reactions and a wide range of (meth)acrylate-based are commercially available [151]. A few examples of most used (meth)acrylate-based monomers and oligomers are depicted in Fig. 4. Other functionalities can also be employed, such as unsaturated polyester, vinyl, vinyl ether, thiol-ene/yne, and even cationic-based systems (in combination with free-radical systems) [152–155]. In general, the selection of suitable monomers or oligomers for vat polymerization is based on the specific application and the processing technology to be used. The main criteria are the resin functionality (mono-, di- or polyfunctional-), viscosity, reaction kinetic, hydrophobicity/hydrophilicity, shrinkage, costs, shelf life, volatility, toxicity, and the final mechanical and functional characteristic of the polymerized product [156]. As photoinitiators, different chemical compounds can be used and can operate in different electromagnetic spectrum wavelengths, e.g., UV, visible, and NIR [157–162]. These compounds can be divided into Type I (unimolecular) and type II (bimolecular) photoinitiators (see Table 2) and have been widely explored in the literature, and most of them can be found commercially [150,163–172]. However, developing more efficient photoinitiators is still of great scientific interest nowadays [173–179]. Free-radical photoinitiators are the most common type of photoinitiators employed in light-based 3D printing. Selecting an appropriate photoinitiator is crucial for the correct production of structures by 3D printing. The absorption spectrum of the photoinitiator must match the emission light from the printer's light source [45]. Other additives can be added to the formulation, e.g., dyes,

reactive diluents or fillers to improve features or functionalities of the printed parts [111,180–187]. Many researchers find VP-3D Printing a flexible technique since, being an open technique, it can be possible to modify or adjust the liquid resin willfully [45,54,188].

In the microfluidic field, VP-3DP found applications some years ago to fabricate templates for PDMS casting for photo-lithography procedures [189,190]. Although this approach led to interesting microfluidic parts, they still present a component of manual labor (not automated) that could introduce high levels of uncertainty or errors in microfluidic assays a posteriori. One of the reasons for using VP-3DP for microfluidic devices fabrication is the possibility of producing microchips in a single step of fabrication (or in the fewest possible steps) [191]. The printable materials used should satisfy some basic criteria in the microfluidic field, e.g., suitable mechanical characteristics, good optical transparency, water/gas permeability and chemical resistance, and low cytotoxicity [156]. Fabricating polymeric 3D printed fluidic devices with all these features is a challenging task that has led to studying several types of printable photopolymers, ranging from commercially available photopolymers to custom-made formulations and performing adequate post-printing protocols on the parts [65,192]. Au et al., in 2014, presented one of the first attempts of using VP-3DP, producing single-step fluidic chips from a commercially available SL-3D printer (3D systems Viper) and the Somos® WaterShed XC 11122 resin (marketed as a suitable resin for obtaining biocompatible and transparent objects). [193]. The researchers produced microfluidic chips with channel dimensions down to 400 μm . Another early try was presented by Prof. Breadmore in 2014 using commercial DLP-based Miicraft (Hsinchu, Taiwan) and a colorless acrylate-based resin (from the printer owner) to fabricate enclosed fluidic devices [194]. The Miicraft is a bottom-up machine that allowed researchers to produce visible transparent microchips within a few minutes, with channel dimensions small as 250 μm and averaging \$1 per chip. These early works probably provided the real starting signal for the effective production of microfluidic devices through VP-3D printing, even the technological limitations faced at that time. Gong et al. developed, in 2015, a mathematical model and performed optical characterization on a customized photopolymer to reach the smallest possible channel dimension into a microfluidic configuration [195]. In this case, the researchers developed their photopolymer based on a low-molecular PEGDA (Mn 250 g/mol), the BAPO photoinitiator (see Table 2) and varying the dye concentration (the Solvent Yellow 14). By setting the appropriate experimental conditions (e.g., light dose, build layer thickness, and resin composition), channel sizes as small as 60 μm x 108 μm were successfully achieved. Later, in 2017, the same researcher group, led by Nordin G.P., continued their studies, achieving flow channels as small as 18 μm x 20 μm , the smallest channel achieved to date (see Fig. 6.a) [27]. In this case, the researchers developed a 385 nm-UV-3D printer and a customized PEGDA-based photopolymer with 2-nitrophenyl phenyl sulfide (NPS) as a dye. The results obtained from these 'preliminary' works led the team to produce microfluidic chips for various applications such as entrapping microparticles (25 μm) inside a microchannels built with pillars and ridged of \sim 30 μm for instance, Fig. 6.b [196], or for the extraction and separation preterm birth (PTB) biomarkers (ferritin) in a microchannel of 45 μm x 50 μm [197]. Parker et al. recently developed microfluidic devices with cross-section channel dimensions of \sim 50 μm for microchip electrophoresis (μCE) separation of various fluorescently labeled amino acids and biomarkers related to the risk of preterm birth (PTB) [198]. By optimizing the conditions of separations (e.g., devices layout, running buffer, and the voltages applied), the yield of separation of the printed devices was comparable to conventional material for microchip electrophoresis analysis with a limit of detection in the high picomolar (pM) to low nanomolar (nM) range; this was another example of how VP-3D printing could effectively be used for microfluidic chip fabrication.

Other important features of microfluidic chips, such as microvalves, micropumps, and another actuator, can also be produced using VP-3D printing. These components can be used to program the fluid flow and create liquid mixtures and gradients during the analysis, sparing the human labor during the tests. Gong et al. demonstrated reported in 2015 the production of 3D printed valves that can be driven pneumatically by willfully deflecting a thin membrane with compressed air and blocking the fluid flow [199]. These actuators were produced using a commercial 3D printer (the B9 Creator printer v1.1) and a lab-made resin based on a low-molecular PEGDA (Mn 250 g/mol), the BAPO photoinitiator and Sudan I dye. The same team improved the stability over time of the valves and pumps, reaching performances up to 1 million of actuation [200]. Besides, the authors optimized the valve's volume (to a tenth of the original design), allowing the production of multiplexers with high-density valves integrated into microfluidic devices. Au and coworkers reported an analogous work, presenting a fully 3D printed valve that could be integrated into microfluidic systems to allow fluids' proper distribution and mixing. The model was fabricated using a commercial resin, the WaterShed XC 11122 photopolymer (marketed as biocompatible and transparent) and the 3D systems Viper SL 3D printer machine set in high-resolution mode. The printed valve consisted of two chambers separated by a thin film or membrane: a control chamber and a fluid chamber. By flushing compressed air in the control chamber, the thin membrane deflects and remains stable, blocking the liquids off with no leaking. As a proof of concept, the research team coupled four printed valves for routing four different liquids into a 3D-printed cell culture chamber, and in this way, CHO-K1 cells were stimulated with ATP solutions, with the possibility to track their Ca²⁺-answer using a fluorescent dye (Fluo-4). The same group presented an article where transparent and biocompatible microfluidic chips arranged with a series of large arrays of valves were cost-affordable produced. In this case, the devices were produced using a customized photopolymer based on a low-molecular-weight (MW=258) monomer and using a commercial DLP-SL 3D printer from Asiga (Pico2-HD, 395 nm) [201].

Researchers have also been focusing more on studying the structure biocompatibility. Takenaga et al. used a commercial printer (PicoPlus 27) from Asiga and a commercial resin from the same company (PlasCLEAR) to 3D-print fluidic systems, presenting an innovative microfluidic assembly method in which the 3D printed fluidic chip is arranged on a light-addressable potentiometric sensor (LAPS) chip made from the same photopolymer. [202] The researchers used these types of assembled devices for Chinese hamster ovary (CHO)-cell growth yielding comparable results to standard cell-culture flasks and giving the possibility to monitor cells' reaction in the channels in real-time. Kuo et al. developed transparent and biocompatible microfluidic chips from a photocurable resin based on low-molecular-weight PEGDA (Mw 250), BAPO photoinitiator and the isopropyl thioxanthone (ITX) photosensitizer [203]. The ITX compound is a Type II photoinitiator that could start the polymerization process in the presence of a co-initiator. However, in Kuo et al.'s work, no co-initiators were added to the resin, and the ITX was used as a UV absorber due to the high molar absorption at 385 nm (the printer's light-emitting source). Besides, ITX neither affected the printed transparency of the microfluidic chips nor introduced unwanted coloration. The transparent chips were printed with the smallest channel width of 500 μm and having surface pillars in the order of a single-pixel (27 μm) and sub-pixel ($\sim 10 \mu\text{m}$). After a post-printing process, the printed chips' biocompatibility was tested, testing the cell viability and proliferation of the Chinese hamster ovary (CHO-K1) with promising results.

Different and interesting works were published presenting 3D printed microfluidic device production for diversified applications. For instance, Wang et al. presented multilayered 3D microfluidic devices for flow-focusing water/oil droplet generation employing a liquid crystal

display (LCD)-based SLA 3D printer [204]. However, the chips were obtained from a commercial acrylate-based resin, Spot-LV from Spot-A. The researcher opted for adding up to 2 wt.% of a green dye into the commercial photopolymer to increase the light-absorbing effect, and thus the printing resolution. They performed various tests (e.g., curing times and printing resolution in each direction) to create microfluidic chips with microchannel of 400 μm (*X-Y plane*) and 800 μm (*Z-axis*), leading to obtaining 3D printed flow-focusing droplet generators that produced droplets with sizes between 50 and 185 μm . Similar work was developed by Männel et al., presenting the production of nonplanar microfluidic flow cell devices for emulsion and polymeric hydrophilic/hydrophobic micro-particle formation [205]. The printed chips were produced through a commercial $\mu\text{SL-3DP}$ (Perfactory P4 mini) and a commercial photopolymer (R11), both from *Envisiontec*. Printing settings such as object-resin vat separation distance, Z-axis building distance, and X-Y plane-light compensation at the edge's stages were adjusted to print precise microfluidic with closed channel sizes down to 75 μm in a single-fabrication step (**Errore. L'origine riferimento non è stata trovata.** see Fig. 6.c). The 3D printed microfluidic chips presented a similar drop-making yield to multi-step PDMS-based flow cell models fabricated by photo- and soft-lithography. Kotz et al. presented a simple method to 3D print microfluidic devices using a commercial printer (Asiga Pico 2) from a custom-made resin based on highly fluorinated (PFPE) methacrylate resin [206]. The authors selected the PFPE photocurable resin due to the high optical transparency and the polymerized parts' high chemical resistance. They opted to add into their resin two types of photoinitiator: TO and BAPO (See Table 2), and various types of light absorbers: Sudan Orange G (SOG), Tinuvin 326 (T326), and Tinuvin 384-2 (T384-2), to achieve the looked-for features. The researchers noted that the photopolymer stability was better using a SOG absorber, which also exhibits an intense absorption in the printer's light-emitting source (about 385 nm), leading to the 3D printing of embedded microfluidic chips (Fig. 6.f). As a result of the fine selection of materials, the 3D printed chips were produced with a channel width of 800 μm and a height of 600 μm as well as with high optical transparency. The printed chip presented excellent resistance toward organic solvents such as dichloromethane (DCM), N, N-dimethylformamide (DMF), tetrahydrofuran (THF) toluene, acetone, and n-heptane. In a curious work, Yeung et al. produced microfluidic chips made of an array of hollow microneedles positioned at the devices' outlet end (Fig. 6.e) [207]. The researchers employed a commercial SL-3D printer (Form2) and a biocompatible material (Dental LT clear), both from FormLab. The devices were designed and printed with three separate inlet microfluidic channels that converge in one 3D spiral chamber. The incoming fluids are hydrodynamically mixed in this last chamber, emerging well-homogenized at the outlet where the microneedles (width between 800 μm and 600 μm , height below 1 mm.) are positioned. Through the channels (2 mm roughly), three-fluorochrome model-drug solutions were injected, and it was observed by ex-vivo confocal microscopy analysis that the developed devices were able to achieve the transdermal drug delivery to porcine skin. The authors reported that such systems might be applied in preclinical drug therapy situations, allowing the in-situ mixing and tuning of multiple drugs. Many works have also been reported utilizing custom-made photopolymers as alternatives to commercial printable materials.

Other interesting works have been reported using lab-made resin based on polydimethylsiloxane (PDMS) reagents as an alternative to conventional PDMS (the Sylgard 184), which is typically used for producing microfluidic chips by casting. Bhattacharjee and coworkers created optically transparent PDMS-based microfluidic devices using a methacrylate-PDMS-based resin and a commercial desktop-SL 3D printer (see Fig. 6.e) [208]. The printed PDMS-based devices presented similar characteristics to the standard Sylgard 184 elastomer and produced chips with

channel dimensions down to 500 μm . Once performed the adequate post-printing washing steps, these devices presented a promising cytocompatibility toward mammalian cell lines. More recently, Zips et al. presented silicone-hydrogel hybrid resins' preparation to produce flexible microfluidic devices with integrated valves, mixers, and chambers through a commercial stereolithography 3D printer [209]. The authors obtained microfluidic structures with internal channels of 450 μm x 500 μm when the printed chip was bonded (top and down) to a glass slide. As a proof of concept, the researchers used their 3D printed silicone-based microfluidic device to cultivate cardiac cells (cardiomyocyte-like HL-1) in a specifically designed chamber inside the printed chip, showing that the cardiac cells retained their electrophysiological activity inside the silicone-based chamber. Our group recently reported the production of complex-shaped PDMS-based fluidic devices by VP-3D printing [210]. The 3D printed chips were produced from a custom-made photopolymer based on acrylate-PDMS, a silicone soluble BAPO-derivate photoinitiator and DR1-MA as a dye, and a commercial DLP-3D printer emitting at 405 nm (Asiga PICO 2). The PDMS-based chips were obtained with good optical features, high chemical stability, good mechanical properties, and microchannels dimensions down to 400 μm x 400 μm . Besides, the microchannel's surfaces were successfully modified, exploiting the required UV-post-curing step by taking advantage of unreacted functional groups after the 3D printing step. In this way, the surface properties of the PDMS-based microdevices were effectively and selectively modified through UV-induced grafting polymerization techniques, giving an added value to the printed devices in terms of surface treatment compared to other methods. Using continuous liquid interface production (CLIP) methods, Berger and coworkers developed microfluidic devices for pathogen detection [211]. The microdevices were produced using RPU70 material and the CLIP-printer Carbon M2. Although with RPU70, one can produce only opaque materials, it is mechanically resistant, chemically stable and compatible with various common solvents, it presents low water absorptivity, and it is biocompatible (according to SO 10993-5/-10) [212]. The authors developed microfluidic devices with open microchannel (or grooves) width and depth small as 400 μm . The 3D printed devices were covered with transparent biocompatible tape, allowing better visualization of the optical imaging during the filling. The printed chips were used to detect *E. Coli* bacteria from whole blood through a loop-mediated isothermal amplification (LAMP) assay with a 50 cfu/ μL limit of detection. The researchers reported a saponin-based lysing approach to process whole blood samples directly in the chip for amplification, which subsequently allowed the portable translation of the assay toward a point-of-a-care (POC) system using a smartphone.

3. 3D printing microfluidic chips: what next?

There are still a few shortcomings that polymeric 3D printing should be overcome to compete with well-established techniques for microchips fabrication and thus be considered a valid technology and not just a promising alternative. The most looked-for characteristics in 3D printed fluidic chips are printing resolution and accuracy, optical transparency, and biocompatibility. Today, current commercial 3D printing resolution is still lower (or poorer) than conventional lithography methods. Most of the published works of 3D-printed microfluidics reported microchannels in the range of 0.5 - 1 mm. Researchers have been looking for novel methods to manufacture truly microfluidic devices (<100 μm). Some researchers achieved sub-millimeter dimension channels using not-so-quite handy and replicable methods. The truth is that these strategies are still highly experimental, and even more technological and material development is needed to converge 3D printing and microfluidic systems entirely.

The FFF method is the 3D printing technique with the highest printing speed (and low initial cost). Using FFF, one common approach is producing sacrificial molds that can be dissolved in a post-3D printing step to develop truly sub-millimeters microfluidic chips (the smallest features 18 μm using a nozzle of 30 μm of diameter) [213]. Though, the typical precision of FFF techniques remains quite above the sub-millimeter features. Photopolymer-based 3D printing methods are considered the best alternative for microfluidic chip manufacturing, as discussed previously. Inkjet 3D printing (i3Dp) presents a better printing resolution than extrusion-based techniques. However, the correct fabrication of sub-microfluidic devices is limited by the supporting material used in the fabrication step. The supporting material can be trapped inside the channels, and it can be quite difficult to remove from the microchannels. In this view, an innovative strategy was presented based on the pausing-and-printing approach by introducing a thin sheet or liquid substances as a physical barrier rather than the conventional supporting material, leading researchers to reach sub-millimeter channel dimensions through i3Dp [122]. However, this method is rather manual and depends on the correct alignment of the physical barrier. Other photopolymer-based techniques, such as the two-photo polymerization (2PP), can easily reach sub-millimeter resolutions; but it requires a considerable initial cost and maintenance. 2PP also has a very slow printing speed and low printing volume compared to other polymeric 3DP technologies. Despite these shortcomings, many researchers have been employing 2PP more as a complementary tool to produce nanometric-scale structures, which can be integrated into microfluidic devices. The idea of producing a single microfluidic device that can be easily handled in laboratories using 2PP is still far from being a reality. This is why the 2PP was not discussed in the previous analysis. With vat polymerization techniques, larger-scale and precise microfluidic chips can be produced faster, though the transversal resolution is still to be improved [211]. The printing resolution of stereolithography and digital light processing 3D printing techniques can reach a few micrometers, although they typically present a lower printing speed than FFF and i3Dp [40].

Beyond printing resolution, another crucial feature for the 3D printing of microfluidic chips is biocompatibility [214–216]. Among the 3D printed techniques discussed in this review, FFF is with the wider commercially available biocompatible materials, as shown in Table 2 [101,102], e.g., polylactic acid (PLA), polymethylmethacrylate (PMMA), polycarbonate (PC), cyclic olefin copolymer (COC), polypropylene (PP), acrylonitrile-butadiene-styrene (ABS) and polyurethane (TPU). These materials can also be found in the market at good prices compared to other materials used for different polymeric 3D printing methods. The situation is slightly different for photopolymerization-based inkjet and Vat polymerization 3D printing. Considering the nature of printable photopolymers, the printed objects frequently contain unreacted chemical products (monomers, photoinitiators, and additives) after the printing step. Such unreacted chemicals can be toxic toward biological entities, hindering the full potential application in the biomedical field [217,218]. Many researchers have reported novel formulations using hydrogels [88,136,219–221]. Hydrogels' main characteristic is their great compatibility with biological entities since they are designed to uptake high water content (> 90 wt.%) [222]. These features make hydrogels a so attractive material for medical, biomedical and pharmaceuticals applications [223,224]. Though, their implementation for microfluidic devices' manufacturing has not been completely adopted because hydrogels could interact undesirably with the fluids flushing through the microchannels, leading to structural changes of the chips [220]. An aspect to consider is that the printed microfluidic devices need to operate with delicate aqueous-based analytes in cell culture or tissue engineering applications [225], which could be solved using hydrogel with partially hydrophobic

characteristics [209]. On the other hand, fluidic platforms made with more dimensionally stable and water-free polymers could enable better performance of microfluidic devices, even if the biocompatibility features are not so great as hydrogels. Recent studies have shown the importance of improving the biocompatibility of such water-free structures [225,226]. In this frame, diverse commercial photopolymers marketed as biocompatible have been reported [205,227]. However, as discussed in the review, only a few studies have been carried out related to the material-biological unit interactions. Most of the studies have been focused on Vat polymerization techniques; for instance, a detailed characterization of four commercial photopolymers (from Formlab) was carried out by Piironen et al., studying their compatibility toward cell lines [228]. The researchers concluded that even if a commercial resin is ISO-certified as biocompatible, it does not imply an adequate cell interaction of the produced parts. They observed that the most crucial point is performing a post-printing procedure on objects to remove the toxic component and improve biocompatibility. Other researchers reached a similar conclusion [229,230]. In all these previous works, the result was common: more attention must be paid to the post-printing procedures to reduce the leaching of toxic compounds from the printed parts.

Even following a post-printing procedure, the lack of detailed information from the supplier about the chemical composition of the resin further complicates the biological studies performance of the printed parts. Herein, the growing interest in developing custom-made photopolymers for 3D printing with biocompatibility features [142,231]. In this line, the idea is to formulate resins to obtain printed parts with adequate biocompatibility and reduced cytotoxicity, which could be foreseen as biocompatible materials for advanced applications after standard treatment validations [54,226]. The development of in-lab and more biocompatible materials, however, could be achieved mainly using vat polymerization techniques owing to their versatility in material preparation (while for i3Dp, producing and implementing in-house materials is hindered by the restriction level of the machines' owners). Interesting work from Nordin's group demonstrated that printed parts (based on PEGDA, Mn 250) were noncytotoxic toward endothelial cells (EA.hy926) even without any post-printing treatment [226]. Männel et al. evaluated the biocompatibility of (meth)acrylate resins toward human umbilical vein endothelial cells (HUVECs) [225]. They tested resins such as PEGMEMA (Mn 500 g/mol), TPGDA (Mn 300.55 g/mol), POEA (Mw 192.21 g/mol) and PEGDA (Mn 575 g/mol). They noticed that a combination of PEGDA and PEGMEMA was the most suitable composition, observing a cell proliferation after five (5) days of culture. Different researchers have explored how the biocompatibility of the printed parts can be increased by removing or reducing the unreacted and potential cytotoxic products by following the appropriate post-printing steps [125,232,233]. Though, the printed objects' bio-functionality can also be enhanced by performing particular post-3D printing protocols not to remove the potentially cytotoxic components from their surface (or "passivation") but by coupling bio-functional groups on their surfaces (or "activation"). These functional groups might be active biological molecules such as antibodies, peptides, nucleic acids, or biocompatible compounds to promote biological interactions like carboxylic acid groups or thiols. As proposed by Männel and coworkers in their work, the bioproperties 3D printed parts might be significantly enhanced if RGD tripeptides are incorporated in the photosensitive resin rather than performing post-printing procedures [225]. By adding Br-containing vinyl-terminated initiator into a commercial UV curable resin, 3D printed objects with modifiable surfaces can be obtained [234]. Such an approach promotes polymer brushes' growth via surface-initiated atom transfer radical polymerization (SI-ATRP) that can be potentially used in the biomedical field. This "activation" strategy could be an interesting path to

follow to introduce functional biomolecules that might enhance the biocompatibility or the bio-interaction of the photopolymerized printed parts with specific biological entities [235].

As seen during this review, interesting use of 3D printed microfluidic chips has been reported. We are in the development phase of 3D printing to manufacture microfluidic devices, with some specific works reporting the biomedical and pharmaceutical application of 3D printed chips [236–240]. Many expectations are still placed on polymer 3D printing due to the flexibility and versatility to simplify and decentralize the micro-manufacturing steps. We might think that polymeric 3D printing will soon meet technological innovations and materials research to bridge current gaps and produce harmonized microfluidic devices for patient-specific treatment, more commonly known as Point-of-a-care (POC) devices. Many researchers have demonstrated the use of polymeric 3D printing to produce microfluidic devices for the patient-specific detection of saliva, urine, and other biological entities. This opens up a myriad of medical applications by combining 3D printing with real medical situations. Low-cost 3D printed microfluidic devices may provide a new avenue for molecular detection at the point of care in resource-limited settings. Over time, it is certainly possible to envision a future where these facilities are shared regionally or nationally, supported by an on-call production team, to improve accessibility to these custom 3D printed and POC devices.

4. Conclusion and future considerations

Polymeric 3D printing is a promising technology that can revolutionize the microfluidic field by introducing faster and cheaper ways to produce microdevices. These technologies, especially FFF, i3Dp and VP-3D printing, are also establishing new strategies for manufacturing such devices, new commercialization approaches, and field of applications. Although the expected potential of 3D printing, it still presents a few shortcomings that should be overcome to compete with well-established conventional techniques for microchips fabrication and thus be considered a valid technology and not just a promising alternative. In this review, an attempt was made to highlight the need to develop and improve the performance of current 3D printing materials and technologies to achieve the great potential of this technology in the production of microfluidic devices in the coming years.

In the next few years, we might expect that the progression of 3D printing will be establishing the pillars to establish this technology as the best alternative for manufacturing microfluidic devices. To achieve such a goal, there is still so much to do in terms of materials and technology development to reach the greatest resolutions, the better precision as possible, the desired optical characteristics, and structures with higher biocompatible features. In recent years, most of the published works are more focused on presenting how polymeric 3D printing could be effectively used for microfluidic fabrication based on studying the characteristics of the machine or using or developing alternative materials. Now, it is time that the 3D printed microfluidics will be used in real microfluidic applications to start to comprehend the possible future scenarios that, in synergy with machines and program progress as well material development, will lead to polymeric 3D printing the expected transformation in the field. Although the utilization of 3D printing has not yet become a central part of standard microfluidic chips today, we anticipate that given the prospects for 3D printing and continuous performance improvement, this technology will be adopted, and more opportunities will progressively emerge for companies and institutions to relevant applications in global health.

Figures

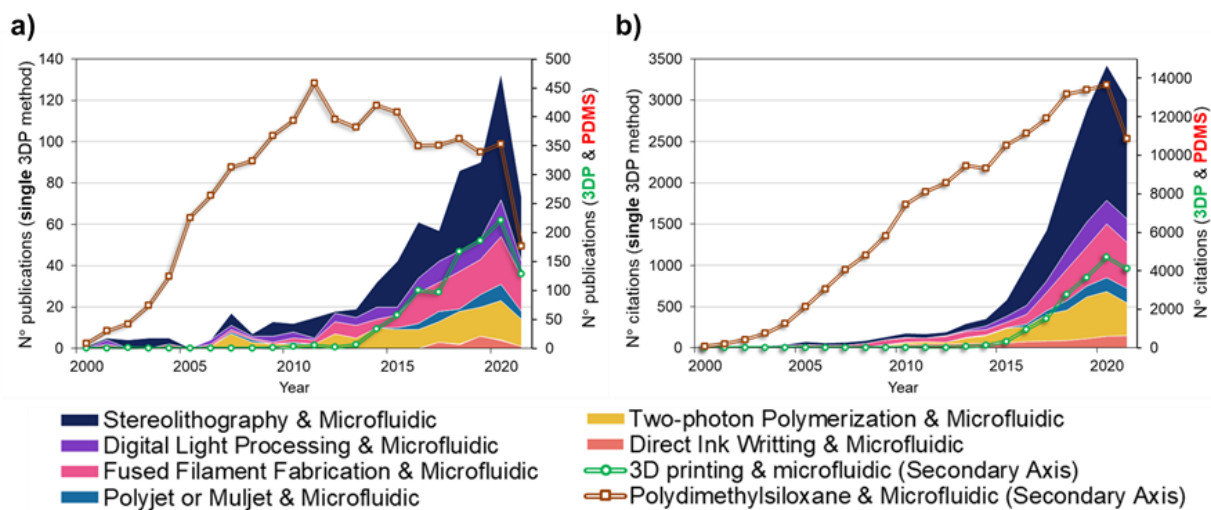


Fig. 1. Statistics data of the (a) Publications and (b) citations per year (from 2001 to 2021) searching by the keywords: “Stereolithography,” “Digital Light Processing,” “Fused Filament Fabrication,” “Polyjet” or “MultiJet,” and “two-photon polymerization” together with “microfluidic.” The terms “3D printing” & “microfluidic” and “Polydimethylsiloxane” & “Microfluidic” were also considered as a point of comparison. Data obtained from the Scopus database, accessed August 11th, 2021.

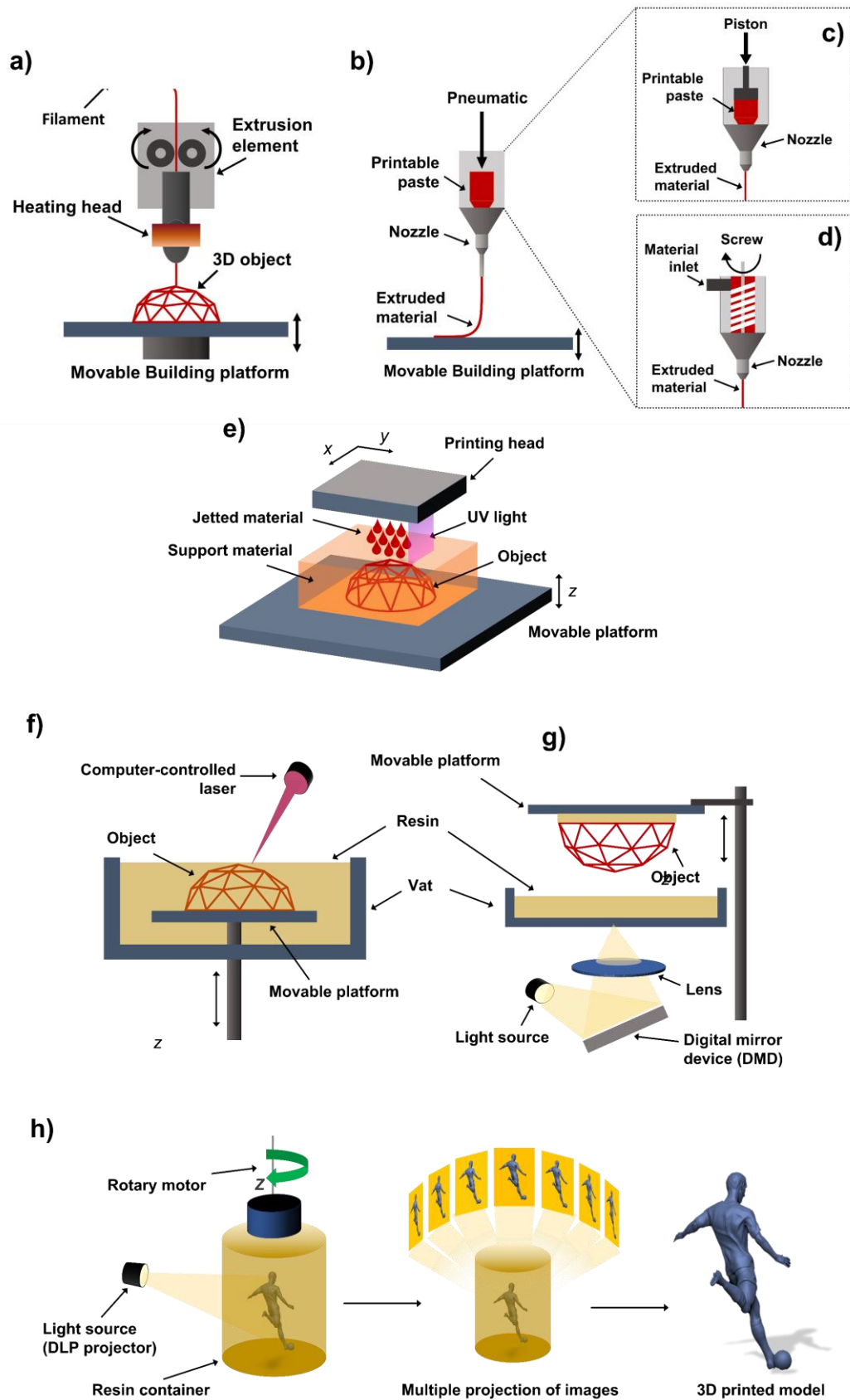


Fig. 2. Representation of (a) Fused filament fabrication (FFF), Direct ink writing based on (b) pneumatic force, (c) a piston and (d) a screw to extrude the material, (e) Photopolymerization-based inkjet 3D printing, (f) Two-photon polymerization, (g) Stereolithography (SL), (h) Digital light processing (DLP) and (i) Computed axial lithography (CAL) methods.

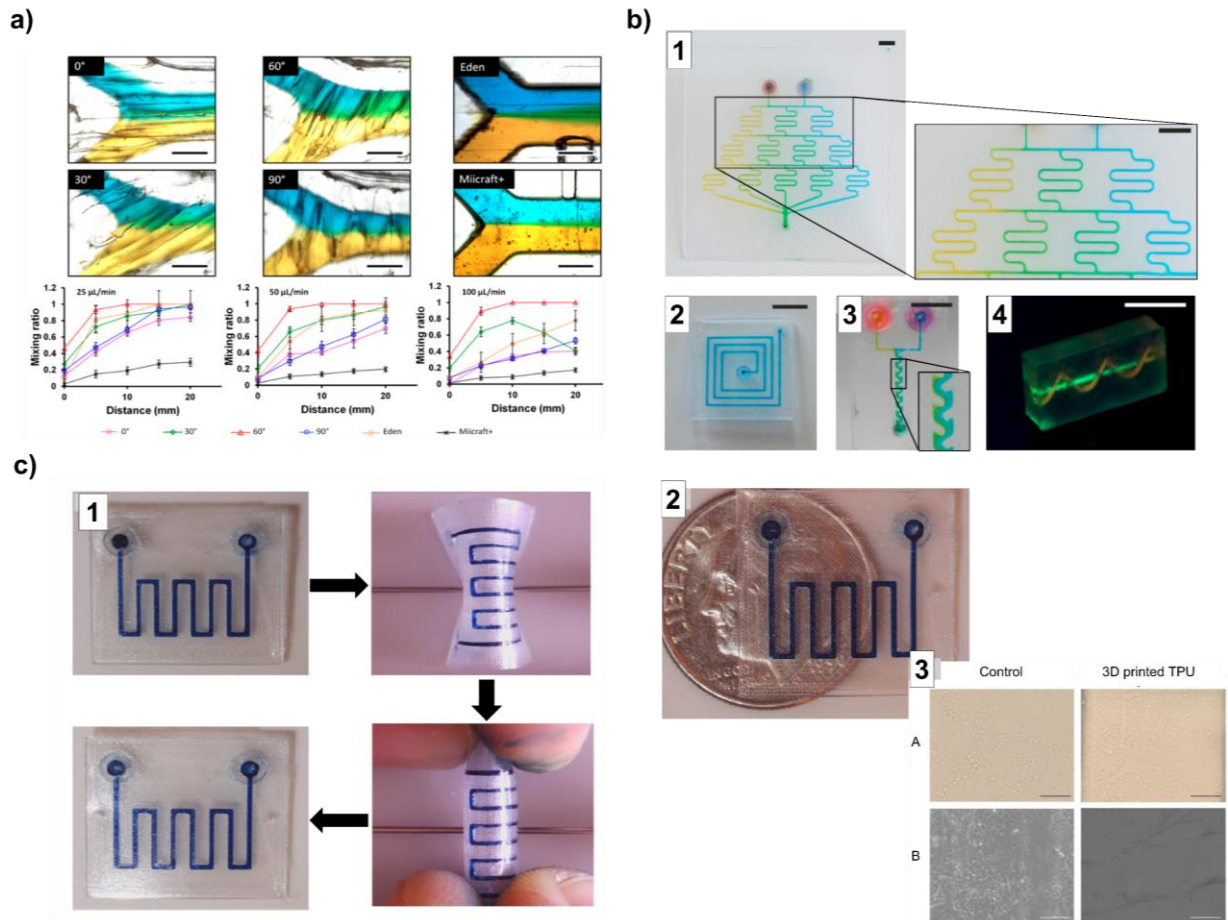


Fig. 3. 3D printed microfluidic chips fabricated by Fused Filament Fabrication (FFF)-3D printing. (a) Microscopic photographs of the laminar fluid flow inside 500 μm x 500 μm channel toward a 750 μm x 500 μm channel, where yellow/blue dyed water is passed through microfluidic channels fabricated by FFF methods at 0°, 30°, 60°, and 90° of filament orientation. The results were compared with chips produced using Eden (Polyjet) and Miicraft+ (DLP-SL) printers. Plots of distance vs. mixing ratio demonstrated the diffusion through the laminar flow channel at 25, 50, and 100 μL/min. (b) 3D printed chips in PMMA: 1) Microchip cascade for mixing yellow/blue-dyed water, 2) chip with a square channel of 600 μm x 600 μm, 3) improved mixer structure of 600 μm x 600 μm channel, and 4) 3D printed serpentine-like channel produced around a straight channel, containing an aqueous fluorescent dye. Images with a scale bar of 10 mm. (c) Transparent 3D printed microfluidic chips made of polyurethane (TPU) images showing 1) the flexibility, 2) the chip transparency, and 3) mIMCD3 cells behavior where a characteristic cobblestone appearance was observed in both, control wells, and 3D printed TPU (scale bars = 100 μm).

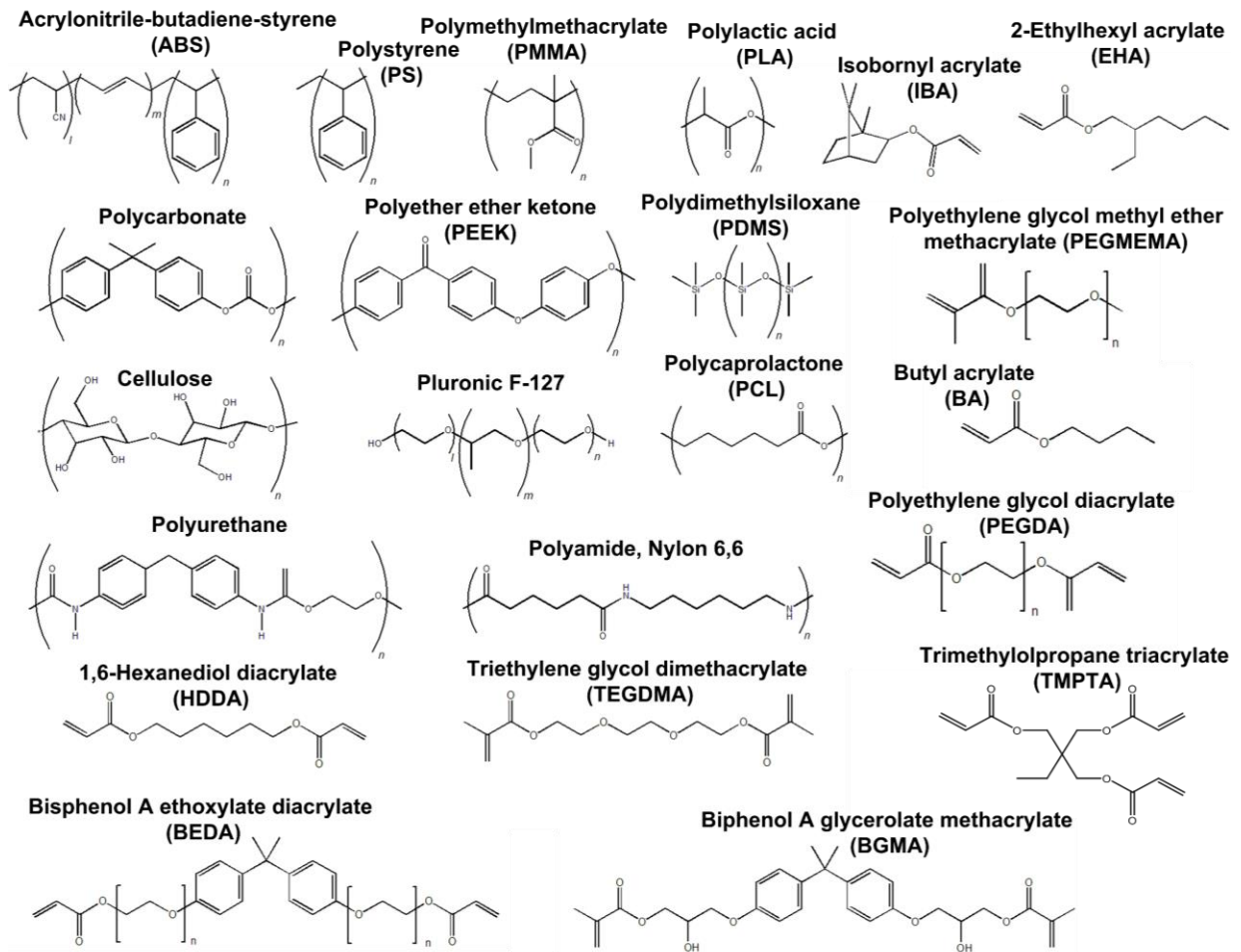


Fig. 4. Chemical structure of some commercially available polymers (thermoplastics and thermosets) used for polymeric 3D printing.

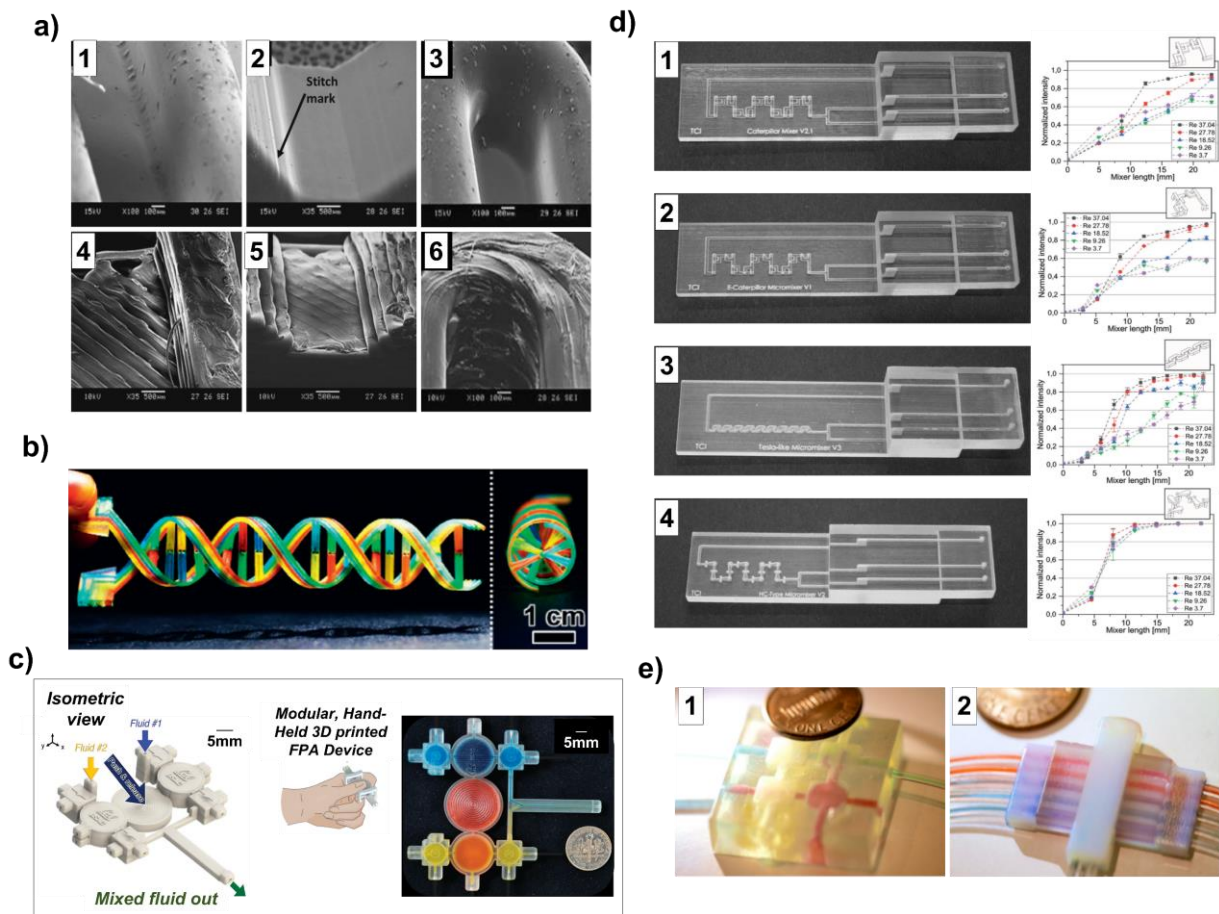


Fig. 5. 3D printed milli- and microfluidic chips fabricated by photopolymer-based inkjet 3D printing methods. (a) Scanning electron microscope (SEM) images of microchannels obtained by i3Dp (1-3) compared to microchannels obtained by FFF (4-6), showing the surface roughness between both techniques. (b) 3D printed DNA-inspired fluidic devices are composed of eight fluidic channels (750 μm in diameter) filled with different dye-colored solutions. (c) Working principle representation of a finger-powered two-fluid FPA prototype for fluid mixing two distinct dyed-colored solutions. (d) Photographs of the 3D printed microfluidic mixers: 1) Caterpillar mixer, 2) enhanced Caterpillar mixer, 3) Tesla-like mixer, and 4) HC mixer. Next to each image is shown the calculated mixing performances (from simulation tests) as a mixer length function. (e) 3D printed microfluidic multichannel valves made of 1) a single material and 2) a multi-material.

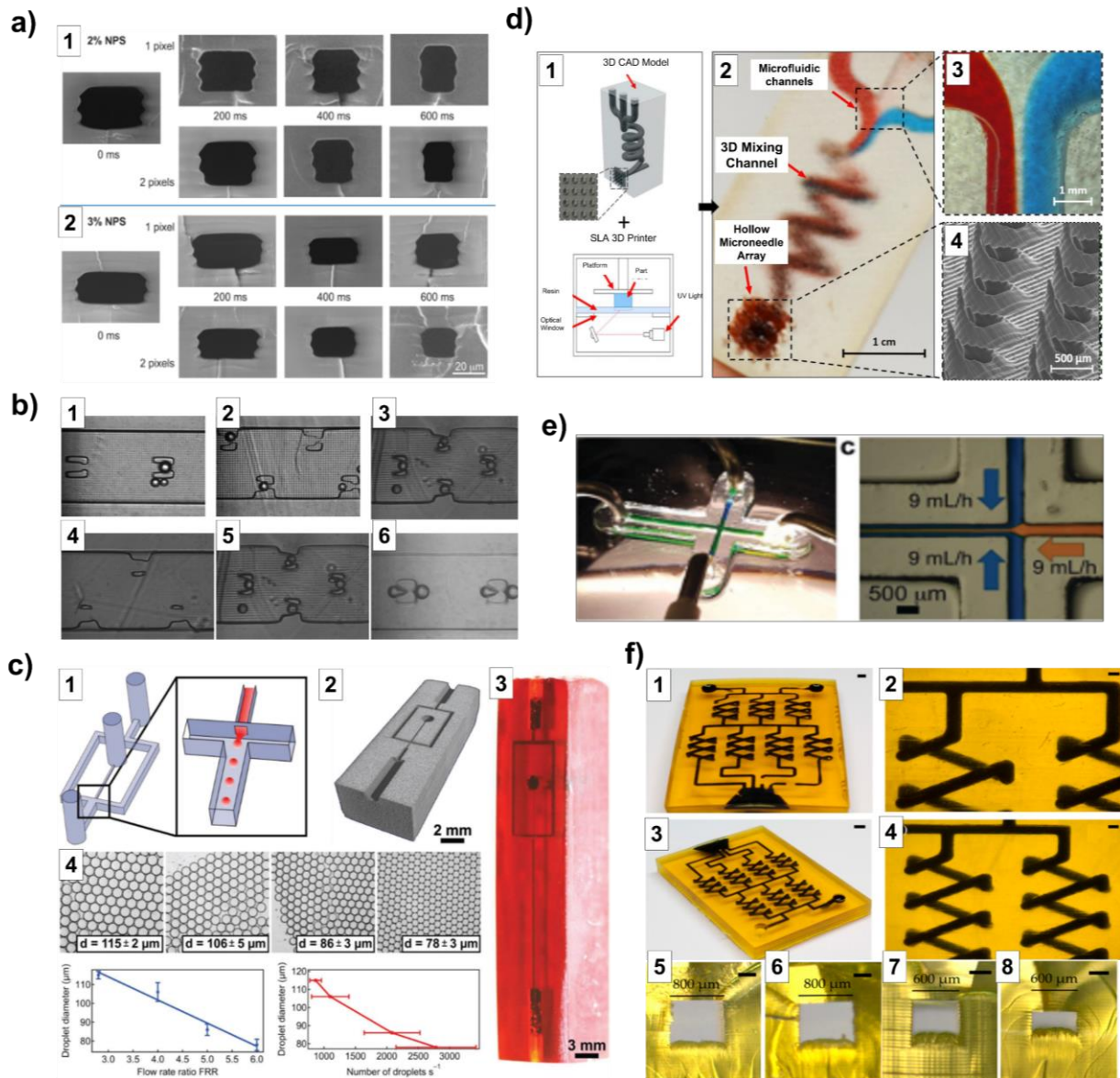


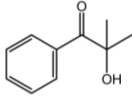
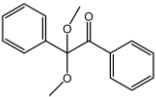
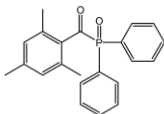
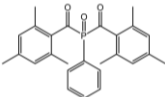
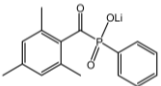
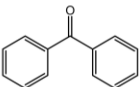
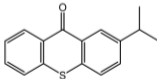
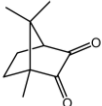
Fig. 6. 3D printed microfluidic chips fabricated by VP-3D printing. (a) 3D printed microchannels (height $\sim 18 \mu\text{m}$) using a custom-made photopolymer based on PEGDA and NPS. (b) Photograph showing the effect of the 3D printed particles trappers positioned at different zones of a microchannel: traps positioned 1) in the center of the channels, 2) staggered along the sides of the channel, 3) staggered along the sides, and in the middle of the channel, 4) traps partially formed after 500 ms of light exposure with no bead capture, 5) particle captured in well-formed traps after 750 ms of exposure, 6) overexposed traps after 1000 ms. (c) Nonplanar 3D printed flow-focusing device: 1) representation of the microfluidic flow cell chip, 2) CAD image of the flow cell model; 3) 3D printed chip using R11 resin, and 4) diameter of the droplet generated vs flow rate ratio (FRR) of dispersed and continuous water-oil phases. (d) 3D printed microfluidic-enabled hollow microneedle devices: 1) CAD design and representation of the process, 2) device composed with 3) three inlets converging into a spiral mixing chamber and a 4) hollow microneedle array outlet. (e) Microfluidic devices from a methacrylate-PDMS-based resin: 1) PDMS-based microfluidic device with $500 \mu\text{m}$ wide channels using a commercial 385 nm SL machine. 2) a central stream of yellow dye (9 mL/h) flanked by two streams of blue dye (9 mL/h each) produces a heterogeneous laminar flow (9 mL h^{-1}) in the fluidic chip. (f) 3D printed perfluoropolyether (PFEP) microfluidic chip: 1) front view of the gradient mixing chip (scale bar: 2 mm) with channel 2) $800 \mu\text{m} \times 800 \mu\text{m}$ filled with black ink (scale bar: $500 \mu\text{m}$), 3) isometric view of the gradient mixing chip (scale bar: 2 mm) with channel 4) $600 \mu\text{m} \times 600 \mu\text{m}$ filled with black ink (scale bar: $500 \mu\text{m}$), 5) lateral view of the $800 \mu\text{m}$ channel width at the inlet and 6) in the middle (scale bar: $250 \mu\text{m}$), 7) lateral view of the $600 \mu\text{m}$ channel width at the inlet and 8) in the middle (scale bar: $250 \mu\text{m}$)

Tables

Table 1. Comparison of the Fused Filament Fabrication (FFF), Polyjet/Multijet and Vat-Polymerization (VP) 3D printing in terms of microfluidic chips fabrication. The table compares the different methods of energy required to join materials (energy source), materials used, minimal printing features, smallest channel achieved, building speed, multi-material ability and pros/cons [38,55,241].

3D printing technique	General characteristics			For microfluidic manufacturing				
	Printing principle	Material	Finest machine resolution	Advantages	Disadvantages	Smallest channel achieved	Benefits	Drawbacks
Fused Filament Fabrication (FFF)	A nozzle gun builds objects by layering softened/melted wires; the objects are then hardened by cooling down	Polylactic acid (PLA), Acrylonitrile-butadiene-styrene (ABS), Polycaprolactone (PCL), Polymethylmethacrylate (PMMA), Polyurethane (PU), Polystyrene (PS), Polycarbonate (PC), Polyether ether ketone (PEEK), cyclic olefin copolymer (COC), polypropylene (PP), polyglycolic acid (PGA), polyethylene terephthalate (PET), Polyamide, polyurethane (TPU)	10-20 μm [73,242]	Low cost; A vast range of processable thermoplastics; simplicity; open-source machines; inexpensive materials; functional objects from common plastics; high printing speed	Low level of precision; Nozzle clogging; anisotropy of the printed parts; only thermoplastics materials; weak mechanical properties; rough finish; weak interlayer bonding	50 μm [95]	Cost-affordable material per printed chip. Some materials present good biocompatibility	Limited printing precision; resolution limited by nozzle diameter; Limited optical transparency; surface roughness might alter fluid flow
Polyjet/Multijet	Jetting of photopolymerizable inks and subsequent curing of the material	Photocurable resins/photopolymers. (meth)acrylate-based; liquid suspensions; elastomers and ceramic-based inks	25 μm [115]	High accuracy, precision, and surface finishing Multi-material/color objects can be obtained	Materials are not so durable in time Sacrificial materials are difficult to recycle Post-processing might damage small features Low mechanical strength	54 μm [122]	Fast printing times, multi-material objects.	Laborious material remotion from the microchannels; No transparency parts; rough surface
Vat polymerization (VP)	Selective curing of liquid resins contained in a vat.	Photocurable resins/photopolymer. (meth)acrylate-based; epoxy; pristine acrylic resins; elastomers and ceramic-based formulations; composites and hybrid photopolymers	0.6-2 μm [243,244]	High accuracy and resolution; using flexible resins; smooth surface finish; versatility on raw material preparation; processing complex nanocomposites	High costs; low printing times; Require support; post-processing to remove support; require post-curing; limited choice of materials; difficult to produce multi-material parts	18 μm [29]	High printing resolution, fast printing chip times, good surface finishing; direct printing of fluidic channels	Post-treatment to remove unreacted material from channels and supports Cytotoxicity Limited materials

Table 2. Most common type I and II free radical photoinitiators for photopolymerization-based 3D printing.

Compound name	Type ^{a)}	Structure	Range of absorption (nm)
2,2-dimethoxy-2-phenylacetophenone (HMMP)	I		(320-360) [245]
2,2-dimethoxy-2-phenylacetophenone (DMPA)	I		(310-370) [246]
Diphenyl(2,4,6-trimethylbenzoyl)-phosphine oxide (TPO)	I		(350-410) [247,248]
phenyl bis (2,4,6-trimethylbenzoyl)-phosphine oxide (BAPO)	I		(360-440) [247]
lithium phenyl-2,4,6-trimethylbenzoyl phosphinate (LAP)	I		(340-400) [249]
Benzophenone	II		(230-280) [250]
2-Isopropylthioxanthone (ITX)	II		(320-400) [251]
Camphorquinone (CQ)	II		(420-490) [252]

^{a)} Type I photoinitiators are compounds that undergo homolytic bond cleavage when absorbing photons, generating two free radicals from Norrish type I reactions and inducing the polymerization process. Type II photoinitiators are uncleavable organic molecules that have a more complex initiating mechanism. These bimolecular photoinitiators, upon light irradiation, can abstract hydrogen atoms from a hydrogen donor to produce excited complexes for initiating the polymerization.

References

- [1] P. Yager, T. Edwards, E. Fu, K. Helton, K. Nelson, M.R. Tam, B.H. Weigl, Microfluidic diagnostic technologies for global public health, *Nature*. 442 (2006) 412–418. <https://doi.org/10.1038/nature05064>.
- [2] E. Verpoorte, Microfluidic chips for clinical and forensic analysis, *Electrophoresis*. 23 (2002) 677–712. [https://doi.org/10.1002/1522-2683\(200203\)23:5<677::AID-ELPS677>3.0.CO;2-8](https://doi.org/10.1002/1522-2683(200203)23:5<677::AID-ELPS677>3.0.CO;2-8).
- [3] C.Y. Lee, C.L. Chang, Y.N. Wang, L.M. Fu, Microfluidic mixing: A review, *Int. J. Mol. Sci.* (2011). <https://doi.org/10.3390/ijms12053263>.
- [4] M. Zhang, C. Xu, L. Jiang, J. Qin, A 3D human lung-on-a-chip model for nanotoxicity testing, *Toxicol. Res. (Camb)*. 7 (2018) 1048–1060. <https://doi.org/10.1039/c8tx00156a>.
- [5] D. Huh, A human breathing lung-on-a-chip, *Ann. Am. Thorac. Soc.* 12 (2015) S42–S44. <https://doi.org/10.1513/AnnalsATS.201410-442MG>.
- [6] D. Huh, Reconstituting Organ-Level Lung, *Science* (80-.). (2010) 1662–1668.
- [7] Y.-H.V. Ma, K. Middleton, L. You, Y. Sun, A review of microfluidic approaches for investigating cancer extravasation during metastasis, *Microsystems Nanoeng.* 4 (2018) 1–13. <https://doi.org/10.1038/micronano.2017.104>.
- [8] A. Bohr, S. Colombo, H. Jensen, Chapter 15 - Future of microfluidics in research and in the market, in: H.A. Santos, D. Liu, H. Zhang (Eds.), *Microfluid. Pharm. Appl.*, William Andrew Publishing, 2019: pp. 425–465. <https://doi.org/https://doi.org/10.1016/B978-0-12-812659-2.00016-8>.
- [9] M. Lake, C. Arciso, K. Cowdrick, T. Storey, S. Zhang, J. Zartman, D. Hoelzle, Microfluidic device design, fabrication, and testing protocols, *Protoc. Exch.* (2015) 1–26. <https://doi.org/10.1038/protex.2015.069>.
- [10] M. Mehling, S. Tay, Microfluidic cell culture, *Curr. Opin. Biotechnol.* 25 (2014) 95–102. <https://doi.org/10.1016/j.copbio.2013.10.005>.
- [11] C.Y. Lee, W.T. Wang, C.C. Liu, L.M. Fu, Passive mixers in microfluidic systems: A review, *Chem. Eng. J.* (2016). <https://doi.org/10.1016/j.cej.2015.10.122>.
- [12] E.A. Mansur, M. YE, Y. WANG, Y. DAI, A State-of-the-Art Review of Mixing in Microfluidic Mixers, *Chinese J. Chem. Eng.* (2008). [https://doi.org/10.1016/S1004-9541\(08\)60114-7](https://doi.org/10.1016/S1004-9541(08)60114-7).
- [13] D. Di Carlo, Inertial microfluidics, *Lab Chip*. 9 (2009) 3038–3046. <https://doi.org/10.1039/b912547g>.
- [14] B.M. Paegel, R.G. Blazej, R.A. Mathies, Microfluidic devices for DNA sequencing: Sample preparation and electrophoretic analysis, *Curr. Opin. Biotechnol.* 14 (2003) 42–50. [https://doi.org/10.1016/S0958-1669\(02\)00004-6](https://doi.org/10.1016/S0958-1669(02)00004-6).
- [15] J. Scott Mellors, K. Jorabchi, L. M. Smith, J. Michael Ramsey, Integrated Microfluidic Device for Automated Single Cell Analysis Using Electrophoretic Separation and Electrospray Ionization Mass Spectrometry, *Anal. Chem.* 82 (2010) 967–973. <https://doi.org/10.1021/ac902218y>.
- [16] S.K. Vashist, P.B. Lippa, L.Y. Yeo, A. Ozcan, J.H.T. Luong, Emerging Technologies for Next-Generation Point-of-Care Testing, *Trends Biotechnol.* 33 (2015) 692–705. <https://doi.org/10.1016/j.tibtech.2015.09.001>.
- [17] G.A. Akceoglu, Y. Saylan, F. Inci, A Snapshot of Microfluidics in Point-of-Care Diagnostics: Multifaceted Integrity with Materials and Sensors, *Adv. Mater. Technol.* 2100049 (2021). <https://doi.org/10.1002/admt.202100049>.

- [18] B.K. Gale, A.R. Jafek, C.J. Lambert, B.L. Goenner, H. Moghimifam, U.C. Nze, S.K. Kamarapu, A review of current methods in microfluidic device fabrication and future commercialization prospects, *Inventions*. 3 (2018). <https://doi.org/10.3390/inventions3030060>.
- [19] A.G. Niculescu, C. Chircov, A.C. Bîrcă, A.M. Grumezescu, Fabrication and applications of microfluidic devices: A review, *Int. J. Mol. Sci.* 22 (2021) 1–26. <https://doi.org/10.3390/ijms22042011>.
- [20] V.I. Vullev, J. Wan, V. Heinrich, P. Landsman, P.E. Bower, B. Xia, B. Millare, G. Jones, Nonlithographic fabrication of microfluidic devices, *J. Am. Chem. Soc.* 128 (2006) 16062–16072. <https://doi.org/10.1021/ja061776o>.
- [21] D. Mark, S. Haeberle, G. Roth, F. Von Stetten, R. Zengerle, Microfluidic Lab-on-a-Chip Platforms: Requirements, Characteristics and Applications, in: S. Kakaç, B. Kosoy, D. Li, A. Pramuanjaroenkij (Eds.), *Microfluid. Based Microsystems*. NATO Sci. Peace Secur. Ser. A Chem. Biol., Springer, Dordrecht, 2010. https://doi.org/10.1007/978-90-481-9029-4_17.
- [22] C. Chen, B.T. Mehl, A.S. Munshi, A.D. Townsend, D.M. Spence, R.S. Martin, 3D-printed microfluidic devices: fabrication, advantages and limitations - a mini review, *Anal. Methods*. (2016). <https://doi.org/10.1039/c6ay01671e>.
- [23] V. Mehta, S.N. Rath, 3D printed microfluidic devices: a review focused on four fundamental manufacturing approaches and implications on the field of healthcare, *Bio-Design Manuf.* (2021). <https://doi.org/10.1007/s42242-020-00112-5>.
- [24] C. Su, Review of 3D-Printed functionalized devices for chemical and biochemical analysis, *Anal. Chim. Acta.* (2021) 338348. <https://doi.org/10.1016/j.aca.2021.338348>.
- [25] F. Zhu, A. Wigh, T. Friedrich, A. Devaux, S. Bony, D. Nugegoda, J. Kaslin, D. Wlodkowic, Automated Lab-on-a-Chip Technology for Fish Embryo Toxicity Tests Performed under Continuous Microperfusion (μ FET), *Environ. Sci. Technol.* 49 (2015) 14570–14578. <https://doi.org/10.1021/acs.est.5b03838>.
- [26] T.M. Valentin, E.M. Dubois, C.E. Machnicki, D. Bhaskar, F.R. Cui, I.Y. Wong, 3D printed self-adhesive PEGDA-PAA hydrogels as modular components for soft actuators and microfluidics, *Polym. Chem.* 10 (2019) 2015–2028. <https://doi.org/10.1039/c9py00211a>.
- [27] H. Gong, B.P. Bickham, A.T. Woolley, G.P. Nordin, Custom 3D printer and resin for 18 μm \times 20 μm microfluidic flow channels, *Lab Chip.* (2017). <https://doi.org/10.1039/C7LC00644F>.
- [28] K. Alessandri, M. Feyeux, B. Gurchenkov, C. Delgado, A. Trushko, K.H. Krause, D. Vignjević, P. Nassoy, A. Roux, A 3D printed microfluidic device for production of functionalized hydrogel microcapsules for culture and differentiation of human Neuronal Stem Cells (hNSC), *Lab Chip.* 16 (2016) 1593–1604. <https://doi.org/10.1039/c6lc00133e>.
- [29] M.J. Beauchamp, G.P. Nordin, A.T. Woolley, Moving from millifluidic to truly microfluidic sub-100- μm cross-section 3D printed devices, *Anal. Bioanal. Chem.* 409 (2017) 4311–4319. <https://doi.org/10.1007/s00216-017-0398-3>.
- [30] T.D. Ngo, A. Kashani, G. Imbalzano, K.T.Q. Nguyen, D. Hui, Additive manufacturing (3D printing): A review of materials, methods, applications and challenges, *Compos. Part B Eng.* 143 (2018). <https://doi.org/10.1016/j.compositesb.2018.02.012>.
- [31] G. Anglani, 3D printed capsules for self-healing concrete applications, (2019). <https://doi.org/10.21012/fc10.235356>.
- [32] D.S. Thomas, S.W. Gilbert, Costs and cost effectiveness of additive manufacturing: A literature review and discussion, in: *Addit. Manuf. Costs, Cost Eff. Ind. Econ.*, 2015.
- [33] F. Matos, R. Godina, C. Jacinto, H. Carvalho, I. Ribeiro, P. Peças, Additive manufacturing: Exploring the social changes and impacts, *Sustain.* (2019). <https://doi.org/10.3390/su11143757>.

- [34] M. Mehrpouya, A. Dehghanhadikolaei, B. Fotovvati, A. Vosooghnia, S.S. Emamian, A. Gisario, The potential of additive manufacturing in the smart factory industrial 4.0: A review, *Appl. Sci.* 9 (2019). <https://doi.org/10.3390/app9183865>.
- [35] M. Gebler, A.J.M. Schoot Uiterkamp, C. Visser, A global sustainability perspective on 3D printing technologies, *Energy Policy*. (2014). <https://doi.org/10.1016/j.enpol.2014.08.033>.
- [36] S. Ford, M. Despeisse, Additive manufacturing and sustainability: an exploratory study of the advantages and challenges, *J. Clean. Prod.* 137 (2016) 1573–1587. <https://doi.org/10.1016/j.jclepro.2016.04.150>.
- [37] D. Chen, S. Heyer, S. Ibbotson, K. Salonitis, J.G. Steingrímsson, S. Thiede, Direct digital manufacturing: Definition, evolution, and sustainability implications, *J. Clean. Prod.* (2015). <https://doi.org/10.1016/j.jclepro.2015.05.009>.
- [38] M. Rafiee, R.D. Farahani, D. Therriault, Multi-Material 3D and 4D Printing: A Survey, *Adv. Sci.* 7 (2020) 1–26. <https://doi.org/10.1002/advs.201902307>.
- [39] D.T. Pham, R.S. Gault, A comparison of rapid prototyping technologies, *Int. J. Mach. Tools Manuf.* 38 (1998) 1257–1287. [https://doi.org/10.1016/S0890-6955\(97\)00137-5](https://doi.org/10.1016/S0890-6955(97)00137-5).
- [40] L.Y. Zhou, J. Fu, Y. He, A Review of 3D Printing Technologies for Soft Polymer Materials, *Adv. Funct. Mater.* 2000187 (2020) 1–38. <https://doi.org/10.1002/adfm.202000187>.
- [41] B.C. Gross, J.L. Erkal, S.Y. Lockwood, C. Chen, D.M. Spence, Evaluation of 3D Printing and Its Potential Impact on Biotechnology and the Chemical Sciences, (2014).
- [42] B. Berman, 3-D printing: The new industrial revolution, *Bus. Horiz.* 55 (2012) 155–162. <https://doi.org/10.1016/j.bushor.2011.11.003>.
- [43] J. Zhao, M. Hussain, M. Wang, Z. Li, N. He, Embedded 3D printing of multi-internal surfaces of hydrogels, *Addit. Manuf.* 32 (2020) 101097. <https://doi.org/10.1016/j.addma.2020.101097>.
- [44] N. Bhattacharjee, A. Urrios, S. Kang, A. Folch, The upcoming 3D-printing revolution in microfluidics, *Lab Chip.* 16 (2016) 1720–1742. <https://doi.org/10.1039/C6LC00163G>.
- [45] J.W. Stansbury, M.J. Idacavage, 3D printing with polymers: Challenges among expanding options and opportunities, *Dent. Mater.* 32 (2016) 54–64. <https://doi.org/10.1016/j.dental.2015.09.018>.
- [46] M. Hofmann, 3D printing gets a boost and opportunities with polymer materials, *ACS Macro Lett.* (2014). <https://doi.org/10.1021/mz4006556>.
- [47] J. Ni, H. Ling, S. Zhang, Z. Wang, Z. Peng, C. Benyshek, R. Zan, A.K. Miri, Z. Li, X. Zhang, J. Lee, K.J. Lee, H.J. Kim, P. Tebon, T. Hoffman, M.R. Dokmeci, N. Ashammakhi, X. Li, A. Khademhosseini, Three-dimensional printing of metals for biomedical applications, *Mater. Today Bio.* 3 (2019). <https://doi.org/10.1016/j.mtbio.2019.100024>.
- [48] R.D. Sochol, E. Sweet, C.C. Glick, S.Y. Wu, C. Yang, M. Restaino, L. Lin, 3D printed microfluidics and microelectronics, *Microelectron. Eng.* 189 (2018) 52–68. <https://doi.org/10.1016/j.mee.2017.12.010>.
- [49] S. Waheed, J.M. Cabot, N.P. Macdonald, T. Lewis, R.M. Guijt, B. Paull, M.C. Breadmore, 3D printed microfluidic devices: enablers and barriers, *Lab Chip.* 16 (2016) 1993–2013. <https://doi.org/10.1039/C6LC00284F>.
- [50] R. Amin, S. Knowlton, A. Hart, B. Yenilmez, F. Ghaderinezhad, S. Katebifar, M. Messina, A. Khademhosseini, S. Tasoglu, 3D-printed microfluidic devices, *Biofabrication.* 8 (2016) 022001. <https://doi.org/10.1088/1758-5090/8/2/022001>.
- [51] C.M.B. Ho, S.H. Ng, K.H.H. Li, Y.-J. Yoon, 3D printed microfluidics for biological applications, *Lab Chip.* 15 (2015) 3627–3637. <https://doi.org/10.1039/C5LC00685F>.

- [52] Q. Yan, H. Dong, J. Su, J. Han, B. Song, Q. Wei, Y. Shi, A Review of 3D Printing Technology for Medical Applications, *Engineering*. 4 (2018) 729–742. <https://doi.org/10.1016/j.eng.2018.07.021>.
- [53] C. Lee Ventola, Medical applications for 3D printing: Current and projected uses, *P T*. 39 (2014) 704–711.
- [54] R.J. Mondschein, A. Kanitkar, C.B. Williams, S.S. Verbridge, T.E. Long, Polymer structure-property requirements for stereolithographic 3D printing of soft tissue engineering scaffolds, *Biomaterials*. 140 (2017) 170–188. <https://doi.org/10.1016/j.biomaterials.2017.06.005>.
- [55] C.M. González-Henríquez, M.A. Sarabia-Vallejos, J. Rodríguez-Hernandez, Polymers for additive manufacturing and 4D-printing: Materials, methodologies, and biomedical applications, *Prog. Polym. Sci.* 94 (2019) 57–116. <https://doi.org/10.1016/j.progpolymsci.2019.03.001>.
- [56] S. V. Murphy, A. Atala, 3D bioprinting of tissues and organs, *Nat. Biotechnol.* 32 (2014) 773–785. <https://doi.org/10.1038/nbt.2958>.
- [57] S. Knowlton, B. Yenilmez, S. Tasoglu, Towards Single-Step Biofabrication of Organs on a Chip via 3D Printing, *Trends Biotechnol.* 34 (2016) 685–688. <https://doi.org/10.1016/j.tibtech.2016.06.005>.
- [58] L. Cavallo, A. Marciandò, M. Cicciù, G. Oteri, 3D Printing beyond Dentistry during COVID 19 Epidemic: A Technical Note for Producing Connectors to Breathing Devices, *Prosthesis*. 2 (2020) 46–52. <https://doi.org/doi:10.3390/prosthesis2020005>.
- [59] R. Tino, R. Moore, S. Antoline, P. Ravi, N. Wake, C.N. Ionita, J.M. Morris, S.J. Decker, A. Sheikh, F.J. Rybicki, L.L. Chepelev, COVID-19 and the role of 3D printing in medicine, *3D Print. Med.* (2020). <https://doi.org/10.1186/s41205-020-00064-7>.
- [60] M. Salmi, J.S. Akmal, E. Pei, J. Wolff, A. Jaribion, S.H. Khajavi, 3D printing in COVID-19: Productivity estimation of the most promising open source solutions in emergency situations, *Appl. Sci.* 10 (2020). <https://doi.org/10.3390/app10114004>.
- [61] S. Ishack, S.R. Lipner, Applications of 3D Printing Technology to Address COVID-19-Related Supply Shortages, *Am. J. Med.* 133 (2020) 771–773. <https://doi.org/https://doi.org/10.1016/j.amjmed.2020.04.002>.
- [62] C. Credi, G. Griffini, M. Levi, S. Turri, Biotinylated Photopolymers for 3D-Printed Unibody Lab-on-a-Chip Optical Platforms, *Small*. 14 (2018) 1–8. <https://doi.org/10.1002/sml.201702831>.
- [63] F. Zhu, N. Macdonald, J. Skommer, D. Wlodkowic, Biological implications of lab-on-a-chip devices fabricated using multi-jet modelling and stereolithography processes, *SPIE Microtechnologies*. 9518 (2015) 951808. <https://doi.org/10.1117/12.2180743>.
- [64] P. Panjan, V. Virtanen, A.M. Sesay, Towards microbioprocess control: An inexpensive 3D printed microbioreactor with integrated online real-Time glucose monitoring, *Analyst*. 143 (2018) 3926–3933. <https://doi.org/10.1039/c8an00308d>.
- [65] G. Weisgrab, A. Ovsianikov, P.F. Costa, Functional 3D Printing for Microfluidic Chips, *Adv. Mater. Technol.* 4 (2019). <https://doi.org/10.1002/admt.201900275>.
- [66] N.P. Macdonald, J.M. Cabot, P. Smejkal, R.M. Guijt, B. Paull, M.C. Breadmore, Comparing Microfluidic Performance of Three-Dimensional (3D) Printing Platforms, *Anal. Chem.* 89 (2017) 3858–3866. <https://doi.org/10.1021/acs.analchem.7b00136>.
- [67] R. Melnikova, A. Ehrmann, K. Finsterbusch, 3D printing of textile-based structures by Fused Deposition Modelling (FDM) with different polymer materials, *IOP Conf. Ser. Mater. Sci. Eng.* 62 (2014). <https://doi.org/10.1088/1757-899X/62/1/012018>.

- [68] J. Emmermacher, D. Spura, J. Cziommer, D. Kilian, T. Wollborn, U. Fritsching, J. Steingroewer, T. Walther, M. Gelinsky, A. Lode, Engineering considerations on extrusion-based bioprinting: interactions of material behavior, mechanical forces and cells in the printing needle, *Biofabrication*. 12 (2020) 025022. <https://doi.org/10.1088/1758-5090/ab7553>.
- [69] S. Vyavahare, S. Teraiya, D. Panghal, S. Kumar, Fused deposition modelling: a review, *Rapid Prototyp. J.* 26 (2020) 176–201. <https://doi.org/10.1108/RPJ-04-2019-0106>.
- [70] S. Crump, Apparatus and method for creating three-dimensional objects - Patent, 1992. https://doi.org/10.2116/bunsekikagaku.28.3_195.
- [71] S. Singh, G. Singh, C. Prakash, S. Ramakrishna, Current status and future directions of fused filament fabrication, *J. Manuf. Process.* 55 (2020) 288–306. <https://doi.org/10.1016/j.jmappro.2020.04.049>.
- [72] I.J. Solomon, P. Sevel, J. Gunasekaran, A review on the various processing parameters in FDM, *Mater. Today Proc.* 37 (2020) 509–514. <https://doi.org/10.1016/j.matpr.2020.05.484>.
- [73] Raise3D, Pro2 Dual Extruder 3D Printer, (2021). <https://www.raise3d.com/pro2/> (accessed August 12, 2021).
- [74] WASP, Delta WASP 2040 become PRO, (n.d.). <https://www.allthat3d.com/fastest-3d-printers/> (accessed August 12, 2021).
- [75] D. Han, H. Lee, ScienceDirect Recent advances in multi-material additive manufacturing: methods and applications, *Curr. Opin. Chem. Eng.* 28 (2020) 158–166. <https://doi.org/10.1016/j.coche.2020.03.004>.
- [76] R.P. Rimington, A.J. Capel, S.D.R. Christie, M.P. Lewis, Biocompatible 3D printed polymers: Via fused deposition modelling direct C2C12 cellular phenotype in vitro, *Lab Chip*. 17 (2017) 2982–2993. <https://doi.org/10.1039/c7lc00577f>.
- [77] E. Nyberg, A. Rindone, A. Dorafshar, W.L. Grayson, Comparison of 3D-Printed Poly-ε-Caprolactone Scaffolds Functionalized with Tricalcium Phosphate, Hydroxyapatite, Bio-Oss, or Decellularized Bone Matrix, *Tissue Eng. - Part A*. (2017). <https://doi.org/10.1089/ten.tea.2016.0418>.
- [78] V. Raeisdasteh Hokmabad, S. Davaran, A. Ramazani, R. Salehi, Design and fabrication of porous biodegradable scaffolds: a strategy for tissue engineering, *J. Biomater. Sci. Polym. Ed.* 28 (2017) 1797–1825. <https://doi.org/10.1080/09205063.2017.1354674>.
- [79] X. Zhang, W. Fan, T. Liu, Fused deposition modeling 3D printing of polyamide-based composites and its applications, *Compos. Commun.* 21 (2020) 100413. <https://doi.org/10.1016/j.coco.2020.100413>.
- [80] J.A. Lewis, Direct ink writing of 3D functional materials, *Adv. Funct. Mater.* 16 (2006) 2193–2204. <https://doi.org/10.1002/adfm.200600434>.
- [81] X. Wan, L. Luo, Y. Liu, J. Leng, Direct Ink Writing Based 4D Printing of Materials and Their Applications, *Adv. Sci.* 7 (2020) 1–29. <https://doi.org/10.1002/advs.202001000>.
- [82] Z. Liu, M. Zhang, B. Bhandari, Y. Wang, 3D printing: Printing precision and application in food sector, *Trends Food Sci. Technol.* 69 (2017) 83–94. <https://doi.org/10.1016/j.tifs.2017.08.018>.
- [83] L. Li, Q. Lin, M. Tang, A.J.E. Duncan, C. Ke, Advanced Polymer Designs for Direct-Ink-Write 3D Printing, *Chem. - A Eur. J.* 25 (2019) 10768–10781. <https://doi.org/10.1002/chem.201900975>.
- [84] Y. Jiang, J. Plog, A.L. Yarin, Y. Pan, Direct ink writing of surface-modified flax elastomer composites, *Compos. Part B Eng.* 194 (2020) 108061.

<https://doi.org/10.1016/j.compositesb.2020.108061>.

- [85] O.D. Yirmibesoglu, L.E. Simonsen, R. Manson, J. Davidson, K. Healy, Y. Menguc, T. Wallin, Multi-material direct ink writing of photocurable elastomeric foams, *Commun. Mater.* 2 (2021). <https://doi.org/10.1038/s43246-021-00186-3>.
- [86] J.A. Lewis, J.E. Smay, J. Stuecker, J. Cesarano, Direct ink writing of three-dimensional ceramic structures, *J. Am. Ceram. Soc.* 89 (2006) 3599–3609. <https://doi.org/10.1111/j.1551-2916.2006.01382.x>.
- [87] N.W.S. Pinargote, A. Smirnov, N. Peretyagin, A. Seleznev, P. Peretyagin, Direct ink writing technology (3d printing) of graphene-based ceramic nanocomposites: A review, *Nanomaterials.* 10 (2020) 1–48. <https://doi.org/10.3390/nano10071300>.
- [88] J. Li, C. Wu, P.K. Chu, M. Gelinsky, 3D printing of hydrogels: Rational design strategies and emerging biomedical applications, *Mater. Sci. Eng. R Reports.* 140 (2020) 100543. <https://doi.org/10.1016/j.mser.2020.100543>.
- [89] V.C.F. Li, C.K. Dunn, Z. Zhang, Y. Deng, H.J. Qi, Direct Ink Write (DIW) 3D Printed Cellulose Nanocrystal Aerogel Structures, *Sci. Rep.* 7 (2017) 1–8. <https://doi.org/10.1038/s41598-017-07771-y>.
- [90] S. Tagliaferri, A. Panagiotopoulos, C. Mattevi, Direct ink writing of energy materials, *Mater. Adv.* 2 (2021) 540–563. <https://doi.org/10.1039/d0ma00753f>.
- [91] L.P. Bressan, T.M. Lima, G.D. da Silveira, J.A.F. da Silva, Low-cost and simple FDM-based 3D-printed microfluidic device for the synthesis of metallic core–shell nanoparticles, *SN Appl. Sci.* 2 (2020) 1–8. <https://doi.org/10.1007/s42452-020-2768-2>.
- [92] L.P. Bressan, J. Robles-Najar, C.B. Adamo, R.F. Quero, B.M.C. Costa, D.P. de Jesus, J.A.F. da Silva, 3D-printed microfluidic device for the synthesis of silver and gold nanoparticles, *Microchem. J.* 146 (2019) 1083–1089. <https://doi.org/10.1016/j.microc.2019.02.043>.
- [93] F. Li, N.P. Macdonald, R.M. Guijt, M.C. Breadmore, Using Printing Orientation for Tuning Fluidic Behavior in Microfluidic Chips Made by Fused Deposition Modeling 3D Printing, *Anal. Chem.* 89 (2017) 12805–12811. <https://doi.org/10.1021/acs.analchem.7b03228>.
- [94] F. Kotz, M. Mader, N. Dellen, P. Risch, A. Kick, D. Helmer, B.E. Rapp, Fused deposition modeling of microfluidic chips in polymethylmethacrylate, *Micromachines.* 11 (2020) 5–8. <https://doi.org/10.3390/mi11090873>.
- [95] M.D. Nelson, N. Ramkumar, B.K. Gale, Flexible, transparent, sub-100 μm microfluidic channels with fused deposition modeling 3D-printed thermoplastic polyurethane, *J. Micromechanics Microengineering.* 29 (2019). <https://doi.org/10.1088/1361-6439/ab2f26>.
- [96] G. Gaal, M. Mendes, T.P. de Almeida, M.H.O. Piazzetta, Â.L. Gobbi, A. Riul, V. Rodrigues, Simplified fabrication of integrated microfluidic devices using fused deposition modeling 3D printing, *Sensors Actuators, B Chem.* 242 (2017) 35–40. <https://doi.org/10.1016/j.snb.2016.10.110>.
- [97] V. Romanov, R. Samuel, M. Chaharlang, A.R. Jafek, A. Frost, B.K. Gale, FDM 3D Printing of High-Pressure, Heat-Resistant, Transparent Microfluidic Devices, *Anal. Chem.* 90 (2018) 10450–10456. <https://doi.org/10.1021/acs.analchem.8b02356>.
- [98] T. Ching, Y. Li, R. Karyappa, A. Ohno, Y.C. Toh, M. Hashimoto, Fabrication of integrated microfluidic devices by direct ink writing (DIW) 3D printing, *Sensors Actuators, B Chem.* 297 (2019) 126609. <https://doi.org/10.1016/j.snb.2019.05.086>.
- [99] M. Athanasiadis, A. Pak, D. Afanassenkau, I.R. Minev, Direct Writing of Elastic Fibers with Optical, Electrical, and Microfluidic Functionality, *Adv. Mater. Technol.* 4 (2019). <https://doi.org/10.1002/admt.201800659>.

- [100] D. Hur, M.G. Say, S.E. Diltemiz, F. Duman, A. Ersöz, R. Say, 3D Micropatterned All-Flexible Microfluidic Platform for Microwave-Assisted Flow Organic Synthesis, *Chempluschem*. 83 (2018) 42–46. <https://doi.org/10.1002/cplu.201700440>.
- [101] F. Li, N.P. Macdonald, R.M. Guijt, M.C. Breadmore, Increasing the functionalities of 3D printed microchemical devices by single material, multimaterial, and print-pause-print 3D printing, *Lab Chip*. 19 (2019) 35–49. <https://doi.org/10.1039/c8lc00826d>.
- [102] M. Kuang, L. Wang, Y. Song, Controllable Printing Droplets for High-Resolution Patterns, *Adv. Mater.* 26 (2014) 6950–6958. <https://doi.org/10.1002/adma.201305416>.
- [103] FacFox documents, PolyJet vs MultiJet Printing(MJP), (2019). <https://facfox.com/docs/kb/polyjet-mjp-comparison> (accessed August 11, 2021).
- [104] H. Gudapati, M. Dey, I. Ozbolat, A comprehensive review on droplet-based bioprinting: Past, present and future, *Biomaterials*. 102 (2016) 20–42. <https://doi.org/10.1016/j.biomaterials.2016.06.012>.
- [105] W.L. Ng, W.Y. Yeong, M.W. Naing, Polyvinylpyrrolidone-based bio-ink improves cell viability and homogeneity during drop-on-demand printing, *Materials (Basel)*. 10 (2017). <https://doi.org/10.3390/ma10020190>.
- [106] Y. Guo, H.S. Patanwala, B. Bognet, A.W.K. Ma, Inkjet and inkjet-based 3D printing: Connecting fluid properties and printing performance, *Rapid Prototyp. J.* 23 (2017) 562–576. <https://doi.org/10.1108/RPJ-05-2016-0076>.
- [107] B. Derby, Bioprinting: Inkjet printing proteins and hybrid cell-containing materials and structures, *J. Mater. Chem.* 18 (2008) 5717–5721. <https://doi.org/10.1039/b807560c>.
- [108] E.M. Kritchman, I. Zeytoun, RAPID PROTOTYPING APPARATUS (US 8.323.017 B2), 2011.
- [109] Y. Yagci, S. Jockusch, N.J. Turro, Photoinitiated polymerization: Advances, challenges, and opportunities, *Macromolecules*. 43 (2010) 6245–6260. <https://doi.org/10.1021/ma1007545>.
- [110] J. V. Crivello, E. Reichmanis, Photopolymer Materials and Processes for Advanced Technologies, (2014).
- [111] M. Gastaldi, F. Cardano, M. Zanetti, G. Viscardi, C. Barolo, S. Bordiga, S. Magdassi, A. Fin, I. Roppolo, Functional Dyes in Polymeric 3D Printing: Applications and Perspectives, (2021). <https://doi.org/10.1021/acsmaterialslett.0c00455>.
- [112] F. Wang, Y. Chong, F.K. Wang, C. He, Photopolymer resins for luminescent three-dimensional printing, *J. Appl. Polym. Sci.* 134 (2017) 1–8. <https://doi.org/10.1002/app.44988>.
- [113] M. Schuster, C. Turecek, B. Kaiser, J. Stampfl, R. Liska, F. Varga, Evaluation of biocompatible photopolymers I: Photoreactivity and mechanical properties of reactive diluents, *J. Macromol. Sci. Part A Pure Appl. Chem.* 44 (2007) 547–557. <https://doi.org/10.1080/10601320701235958>.
- [114] M. Sugavaneswaran, G. Arumaikkannu, Analytical and experimental investigation on elastic modulus of reinforced additive manufactured structure, *Mater. Des.* 66 (2015) 29–36. <https://doi.org/10.1016/j.matdes.2014.10.029>.
- [115] S.C. Ligon, R. Liska, J. Stampfl, M. Gurr, R. Mülhaupt, Polymers for 3D Printing and Customized Additive Manufacturing, *Chem. Rev.* 117 (2017) 10212–10290. <https://doi.org/10.1021/acs.chemrev.7b00074>.
- [116] N. Vidakis, M. Petousis, N. Vaxevanidis, J. Kechagias, Surface Roughness Investigation of PolyJet 3D Printing, *Mathematics*. 8 (2020) 1758. <https://doi.org/10.3390/math8101758>.
- [117] J.M. Lee, M. Zhang, W.Y. Yeong, Characterization and evaluation of 3D printed microfluidic chip for cell processing, *Microfluid. Nanofluidics*. 20 (2016) 1–15.

<https://doi.org/10.1007/s10404-015-1688-8>.

- [118] R.D. Sochol, E. Sweet, C.C. Glick, S. Venkatesh, A. Avetisyan, K.F. Ekman, A. Raulinaitis, A. Tsai, A. Wienkers, K. Korner, K. Hanson, A. Long, B.J. Hightower, G. Slatton, D.C. Burnett, T.L. Massey, K. Iwai, L.P. Lee, K.S.J. Pister, L. Lin, 3D printed microfluidic circuitry via multijet-based additive manufacturing, *Lab Chip*. 16 (2016) 668–678. <https://doi.org/10.1039/c5lc01389e>.
- [119] E. Sweet, R. Mehta, Y. Xu, R. Jew, R. Lin, L. Lin, Finger-powered fluidic actuation and mixing: Via Multijet 3D printing, *Lab Chip*. 20 (2020) 3375–3385. <https://doi.org/10.1039/d0lc00488j>.
- [120] R. Walczak, K. Adamski, W. Kubicki, Inkjet 3D printed chip for capillary gel electrophoresis, *Sensors Actuators, B Chem.* 261 (2018) 474–480. <https://doi.org/10.1016/j.snb.2018.01.174>.
- [121] A. Enders, I.G. Siller, K. Urmann, M.R. Hoffmann, J. Bahnemann, 3D Printed Microfluidic Mixers—A Comparative Study on Mixing Unit Performances, *Small*. 15 (2019) 1–9. <https://doi.org/10.1002/smll.201804326>.
- [122] A.D. Castiaux, C.W. Pinger, E.A. Hayter, M.E. Bunn, R.S. Martin, D.M. Spence, PolyJet 3D-Printed Enclosed Microfluidic Channels without Photocurable Supports, *Anal. Chem.* (2019). <https://doi.org/10.1021/acs.analchem.9b01302>.
- [123] A.M. Tohill, M. Partridge, S.W. James, R.P. Tatam, Fabrication and optimisation of a fused filament 3D-printed microfluidic platform, *J. Micromechanics Microengineering*. 27 (2017). <https://doi.org/10.1088/1361-6439/aa5ae3>.
- [124] S.J. Keating, M.I. Gariboldi, W.G. Patrick, S. Sharma, D.S. Kong, N. Oxman, 3D printed multimaterial microfluidic valve, *PLoS One*. 11 (2016) 1–12. <https://doi.org/10.1371/journal.pone.0160624>.
- [125] W.L. Ng, J.M. Lee, M. Zhou, Y.W. Chen, K.X.A. Lee, W.Y. Yeong, Y.F. Shen, Vat polymerization-based bioprinting - process, materials, applications and regulatory challenges, *Biofabrication*. 12 (2020). <https://doi.org/10.1088/1758-5090/ab6034>.
- [126] W. Li, L.S. Mille, J.A. Robledo, T. Uribe, V. Huerta, Y.S. Zhang, Recent Advances in Formulating and Processing Biomaterial Inks for Vat Polymerization-Based 3D Printing, *Adv. Healthc. Mater.* 9 (2020) 1–18. <https://doi.org/10.1002/adhm.202000156>.
- [127] F.P.W. Melchels, J. Feijen, D.W. Grijpma, A review on stereolithography and its applications in biomedical engineering, *Biomaterials*. 31 (2010) 6121–6130. <https://doi.org/10.1016/j.biomaterials.2010.04.050>.
- [128] R.D. Farahani, M. Dubé, D. Therriault, Three-Dimensional Printing of Multifunctional Nanocomposites: Manufacturing Techniques and Applications, *Adv. Mater.* (2016) 5794–5821. <https://doi.org/10.1002/adma.201506215>.
- [129] M.G. Guerra, C. Volpone, L.M. Galantucci, G. Percoco, Photogrammetric measurements of 3D printed microfluidic devices, *Addit. Manuf.* 21 (2018) 53–62. <https://doi.org/10.1016/j.addma.2018.02.013>.
- [130] H. Kodama, Automatic method for fabricating a three-dimensional plastic model with photo-hardening polymer, *Rev. Sci. Instrum.* (1981). <https://doi.org/10.1063/1.1136492>.
- [131] C.W. Hull, Apparatus for Production of Three-Dimensional Objects By Stereolithography, Patent. (1984) 16.
- [132] A. Oesterreicher, J. Wiener, M. Roth, A. Moser, R. Gmeiner, M. Edler, G. Pinter, T. Griesser, Tough and degradable photopolymers derived from alkyne monomers for 3D printing of biomedical materials, *Polym. Chem.* (2016). <https://doi.org/10.1039/c6py01132b>.

- [133] K. Ikuta, K. Hirowatari, Real three dimensional micro fabrication using stereo lithography and metal molding, in: Proc. IEEE Micro Electro Mech. Syst., Fort Lauderdale, FL, USA, 1993: pp. 42–27. <https://doi.org/10.1109/MEMSYS.1993.296949>.
- [134] J. DeSimone, E. Sarnulski, A. Ermoshkin, P. DeSimone, Rapid 3D Continuous Printing of Casting Molds for Metals and Other Materials, WO 2015/080888A2, 2015.
- [135] H. Quan, T. Zhang, H. Xu, S. Luo, J. Nie, X. Zhu, Photo-curing 3D printing technique and its challenges, *Bioact. Mater.* (2020). <https://doi.org/10.1016/j.bioactmat.2019.12.003>.
- [136] J.F. Xing, M.L. Zheng, X.M. Duan, Two-photon polymerization microfabrication of hydrogels: an advanced 3D printing technology for tissue engineering and drug delivery, *Chem. Soc. Rev.* (2015). <https://doi.org/10.1039/c5cs00278h>.
- [137] I. Bhattacharya, B. Kelly, M. Shusteff, C. Spadaccini, H. Taylor, Computed axial lithography: volumetric 3D printing of arbitrary geometries (Conference Presentation), in: 2018. <https://doi.org/10.1117/12.2307780>.
- [138] H. Li, W. Fan, X. Zhu, Three-dimensional printing: The potential technology widely used in medical fields, *J. Biomed. Mater. Res. - Part A.* (2020). <https://doi.org/10.1002/jbm.a.36979>.
- [139] P. Juskova, A. Ollitrault, M. Serra, J.L. Viovy, L. Malaquin, Resolution improvement of 3D stereo-lithography through the direct laser trajectory programming: Application to microfluidic deterministic lateral displacement device, *Anal. Chim. Acta.* (2018). <https://doi.org/10.1016/j.aca.2017.11.062>.
- [140] Y. Liu, Q. Hu, F. Zhang, C. Tuck, D. Irvine, R. Hague, Y. He, M. Simonelli, G.A. Rance, E.F. Smith, R.D. Wildman, Additive manufacture of three dimensional nanocomposite based objects through multiphoton fabrication, *Polymers (Basel)*. 8 (2016) 325. <https://doi.org/10.3390/polym8090325>.
- [141] Y.-L. Cheng, H.-L. Kao, Study on visible-light-curable polycaprolactone and poly(ethylene glycol) diacrylate for LCD-projected maskless additive manufacturing system, in: *Light Manip. Org. Mater. Devices II*, 2015. <https://doi.org/10.1117/12.2188047>.
- [142] S.H. Kim, Y.K. Yeon, J.M. Lee, J.R. Chao, Y.J. Lee, Y.B. Seo, M.T. Sultan, O.J. Lee, J.S. Lee, S. Il Yoon, I.S. Hong, G. Khang, S.J. Lee, J.J. Yoo, C.H. Park, Precisely printable and biocompatible silk fibroin bioink for digital light processing 3D printing, *Nat. Commun.* 9 (2018) 1–14. <https://doi.org/10.1038/s41467-018-03759-y>.
- [143] C. Yu, J. Schimelman, P. Wang, K.L. Miller, X. Ma, S. You, J. Guan, B. Sun, W. Zhu, S. Chen, Photopolymerizable Biomaterials and Light-Based 3D Printing Strategies for Biomedical Applications, *Chem. Rev.* (2020). <https://doi.org/10.1021/acs.chemrev.9b00810>.
- [144] A.K. Nguyen, R.J. Narayan, Two-photon polymerization for biological applications, *Mater. Today.* (2017). <https://doi.org/10.1016/j.mattod.2017.06.004>.
- [145] R. Infuehr, J. Stampfl, S. Krivec, R. Liska, H. Lichtenegger, V. Satzinger, V. Schmidt, N. Matsko, W. Grogger, 3D-structuring of optical waveguides with two photon polymerization, *MRS Proc.* 1179 (2009) 1179-BB01-07. <https://doi.org/10.1557/PROC-1179-BB01-07>.
- [146] R. Whitby, Y. Ben-Tal, R. MacMillan, S. Janssens, S. Raymond, D. Clarke, J. Jin, A. Kay, M.C. Simpson, Photoinitiators for two-photon polymerisation: effect of branching and viscosity on polymerisation thresholds, *RSC Adv.* 7 (2017) 13232–13239. <https://doi.org/10.1039/c6ra27176f>.
- [147] B.E. Kelly, I. Bhattacharya, H. Heidari, M. Shusteff, C.M. Spadaccini, H.K. Taylor, Volumetric additive manufacturing via tomographic reconstruction, *Science (80-.)*. (2019). <https://doi.org/10.1126/science.aau7114>.
- [148] B.E. Kelly, I. Bhattacharya, M. Shusteff, H.K. Taylor, C.M. Spaddacini, Computed axial lithography for rapid volumetric 3D additive manufacturing, in: *Solid Free. Fabr. 2017 Proc.*

28th Annu. Int. Solid Free. Fabr. Symp. - An Addit. Manuf. Conf. SFF 2017, 2020.

- [149] P.N. Bernal, P. Delrot, D. Loterie, Y. Li, J. Malda, C. Moser, R. Levato, Biofabrication: Volumetric Bioprinting of Complex Living-Tissue Constructs within Seconds (Adv. Mater. 42/2019), Adv. Mater. (2019). <https://doi.org/10.1002/adma.201970302>.
- [150] J.P. Fouassier, J. Lalevée, Photoinitiators for Polymer Synthesis, 2012. <https://doi.org/10.1002/9783527648245>.
- [151] B. Narupai, A. Nelson, 100th Anniversary of Macromolecular Science Viewpoint: Macromolecular Materials for Additive Manufacturing, ACS Macro Lett. (2020) 627–638. <https://doi.org/10.1021/acsmacrolett.0c00200>.
- [152] J. Lammel-Lindemann, I.A. Dourado, J. Shanklin, C.A. Rodriguez, L.H. Catalani, D. Dean, Photocrosslinking-based 3D printing of unsaturated polyesters from isosorbide: A new material for resorbable medical devices, Bioprinting. (2020). <https://doi.org/10.1016/j.bprint.2019.e00062>.
- [153] P.J. Scott, V. Meenakshisundaram, M. Hegde, C.R. Kasprzak, C.R. Winkler, K.D. Feller, C.B. Williams, T.E. Long, 3D Printing Latex: A Route to Complex Geometries of High Molecular Weight Polymers, ACS Appl. Mater. Interfaces. (2020). <https://doi.org/10.1021/acsam.9b19986>.
- [154] H. Leonards, S. Engelhardt, A. Hoffmann, L. Pongratz, S. Schriever, J. Bläsius, M. Wehner, A. Gillner, Advantages and drawbacks of Thiol-ene based resins for 3D-printing, in: Laser 3D Manuf. II, 2015. <https://doi.org/10.1117/12.2081169>.
- [155] T. Zhao, X. Li, R. Yu, Y. Zhang, X. Yang, X. Zhao, L. Wang, W. Huang, Silicone-Epoxy-Based Hybrid Photopolymers for 3D Printing, Macromol. Chem. Phys. 219 (2018) 1–10. <https://doi.org/10.1002/macp.201700530>.
- [156] A. Bagheri, J. Jin, Photopolymerization in 3D Printing, ACS Appl. Polym. Mater. 1 (2019) 593–611. <https://doi.org/10.1021/acsapm.8b00165>.
- [157] S. Shanmugam, J. Xu, C. Boyer, Light-regulated polymerization under near-infrared/far-red irradiation catalyzed by bacteriochlorophyll a, Angew. Chemie - Int. Ed. (2016). <https://doi.org/10.1002/anie.201510037>.
- [158] N. Corrigan, J. Xu, C. Boyer, A Photoinitiation System for Conventional and Controlled Radical Polymerization at Visible and NIR Wavelengths, Macromolecules. (2016). <https://doi.org/10.1021/acs.macromol.6b00542>.
- [159] A. Al Mousawi, C. Poriel, F. Dumur, J. Toufaily, T. Hamieh, J.P. Fouassier, J. Lalevée, Zinc Tetraphenylporphyrin as High Performance Visible Light Photoinitiator of Cationic Photosensitive Resins for LED Projector 3D Printing Applications, Macromolecules. (2017). <https://doi.org/10.1021/acs.macromol.6b02596>.
- [160] J. Xu, S. Shanmugam, C. Fu, K.F. Aguey-Zinsou, C. Boyer, Selective Photoactivation: From a Single Unit Monomer Insertion Reaction to Controlled Polymer Architectures, J. Am. Chem. Soc. (2016). <https://doi.org/10.1021/jacs.5b12408>.
- [161] B.M. Hong, S.A. Park, W.H. Park, Effect of photoinitiator on chain degradation of hyaluronic acid, Biomater. Res. (2019). <https://doi.org/10.1186/s40824-019-0170-1>.
- [162] J. Zhang, J. Lalevée, J. Zhao, B. Graff, M.H. Stenzel, P. Xiao, Dihydroxyanthraquinone derivatives: Natural dyes as blue-light-sensitive versatile photoinitiators of photopolymerization, Polym. Chem. (2016). <https://doi.org/10.1039/c6py01550f>.
- [163] F. Masson, C. Decker, S. Andre, X. Andrieu, UV-curable formulations for UV-transparent optical fiber coatings: I. Acrylic resins, Prog. Org. Coatings. 49 (2004) 1–12. [https://doi.org/10.1016/S0300-9440\(03\)00122-X](https://doi.org/10.1016/S0300-9440(03)00122-X).

- [164] Y.H. Wang, P. Wan, Ketoprofen as a photoinitiator for anionic polymerization, *Photochem. Photobiol. Sci.* (2015). <https://doi.org/10.1039/c4pp00454j>.
- [165] M. Stemmelen, F. Pessel, V. Lapinte, S. Caillol, J.P. Habas, J.J. Robin, A fully biobased epoxy resin from vegetable oils: From the synthesis of the precursors by thiol-ene reaction to the study of the final material, *J. Polym. Sci. Part A Polym. Chem.* 49 (2011) 2434–2444. <https://doi.org/10.1002/pola.24674>.
- [166] A. Ravve, *Light-Associated Reactions of Synthetic Polymers*, Springer US, 2006.
- [167] A. Santini, I.T. Gallegos, C.M. Felix, Photoinitiators in dentistry: a review., *Prim. Dent. J.* (2013). <https://doi.org/10.1308/205016814809859563>.
- [168] I. Kunio, E. Takeshi, A review of the development of radical photopolymerization initiators used for designing light-curing dental adhesives and resin composites, *Dent. Mater. J.* (2010). <https://doi.org/10.4012/dmj.2009-137>.
- [169] J. Lalevée, F. Morlet-Savary, C. Dietlin, B. Graff, J.P. Fouassier, Photochemistry and radical chemistry under low intensity visible light sources: Application to photopolymerization reactions, *Molecules.* (2014). <https://doi.org/10.3390/molecules190915026>.
- [170] M. Kaur, A.K. Srivastava, Photopolymerization: A review, *J. Macromol. Sci. - Polym. Rev.* (2002). <https://doi.org/10.1081/MC-120015988>.
- [171] C. Kutall, P.A. Grutsch, D.B. Yang, A novel strategy for photoinitiated anionic-polymerization, *Macromolecules.* 24 (1991) 6872–6873. <https://doi.org/10.1021/ma00026a016>.
- [172] B.J. Palmer, C. Kutal, R. Billing, H. Hening, A new photoinitiator for anionic-polymerization, *Macromolecules.* 28 (1995) 1328–1329. <https://doi.org/10.1021/ma00108a078>.
- [173] M. Rahal, H. Mokbel, B. Gra, J. Toufaily, T. Hamieh, J. Lalev, Mono vs. Difunctional Coumarin as Photoinitiators in Photocomposite Synthesis and 3D Printing, *Catalysts.* 10 (2020) 1–18. <https://doi.org/doi:10.3390/catal10101202>.
- [174] A.K. Nguyen, P.L. Goering, R.K. Elespuru, S.S. Das, R.J. Narayan, The photoinitiator lithium phenyl (2,4,6-Trimethylbenzoyl) phosphinate with exposure to 405 nm light is cytotoxic to mammalian cells but not mutagenic in bacterial reverse mutation assays, *Polymers (Basel).* 12 (2020) 1–13. <https://doi.org/10.3390/polym12071489>.
- [175] W. Tomal, J. Ortyl, Water-soluble photoinitiators in biomedical applications, *Polymers (Basel).* 12 (2020) 1–30. <https://doi.org/10.3390/POLYM12051073>.
- [176] T.N. Eren, T. Gencoglu, M. Abdallah, J. Lalevée, D. Avci, A water soluble and highly reactive bisphosphonate functionalized thioxanthone-based photoinitiator, *Eur. Polym. J.* 135 (2020) 109906. <https://doi.org/10.1016/j.eurpolymj.2020.109906>.
- [177] L. Breloy, C. Negrell, A.S. Mora, W.S.J. Li, V. Brezová, S. Caillol, D.L. Versace, Vanillin derivative as performing type I photoinitiator, *Eur. Polym. J.* 132 (2020) 109727. <https://doi.org/10.1016/j.eurpolymj.2020.109727>.
- [178] D.M. Love, B.D. Fairbanks, C.N. Bowman, Evaluation of Aromatic Thiols as Photoinitiators, *Macromolecules.* 53 (2020) 5237–5247. <https://doi.org/10.1021/acs.macromol.0c00757>.
- [179] S. Liu, H. Chen, Y. Zhang, K. Sun, Y. Xu, F. Morlet-Savary, B. Graff, G. Noirbent, C. Pigot, D. Brunel, M. Nechab, D. Gimes, P. Xiao, F. Dumur, J. Lalevée, Monocomponent photoinitiators based on benzophenone-carbazole structure for LED photoinitiating systems and application on 3D printing, *Polymers (Basel).* 12 (2020) 1–15. <https://doi.org/10.3390/polym12061394>.
- [180] R. Ni, B. Qian, C. Liu, X. Liu, J. Qiu, Three-dimensional printing of hybrid organic/inorganic composites with long persistence luminescence, *Opt. Mater. Express.* 8 (2018) 2823–2831. [https://doi.org/10.1016/S0920-9964\(12\)70638-2](https://doi.org/10.1016/S0920-9964(12)70638-2).

- [181] J. Palaganas, A.C. de Leon, J. Mangadlao, N. Palaganas, A. Mael, Y.J. Lee, H.Y. Lai, R. Advincula, Facile Preparation of Photocurable Siloxane Composite for 3D Printing, *Macromol. Mater. Eng.* 302 (2017) 1–9. <https://doi.org/10.1002/mame.201600477>.
- [182] C.M. González-Henríquez, G. del C. Pizarro, M.A. Sarabia-Vallejos, C.A. Terraza, Z.E. López-Cabaña, In situ-preparation and characterization of silver-HEMA/PEGDA hydrogel matrix nanocomposites: Silver inclusion studies into hydrogel matrix, *Arab. J. Chem.* (2014). <https://doi.org/10.1016/j.arabjc.2014.11.012>.
- [183] E.T. Tenório-Neto, M.R. Guilherme, M.E.G. Winkler, L. Cardozo-Filho, S.C. Beneti, A.F. Rubira, M.H. Kunita, Synthesis and characterization of silver nanoparticle nanocomposite thin films with thermally induced surface morphology changes, *Mater. Lett.* 159 (2015) 118–121. <https://doi.org/10.1016/j.matlet.2015.06.095>.
- [184] V. Jankauskaite, A. Lazauskas, E. Gri Konis, A. Lisauskaite, K. Ukiene, UV-curable aliphatic silicone acrylate organic–inorganic hybrid coatings with antibacterial activity, *Molecules.* 22 (2017). <https://doi.org/10.3390/molecules22060964>.
- [185] Y.-C. Chen, T.-Y. Liu, Y.-H. Li, Photoreactivity study of photoinitiated free radical polymerization using Type II photoinitiator containing thioxanthone initiator as a hydrogen acceptor and various amine-type co-initiators as hydrogen donors, *J. Coatings Technol. Res.* (2020). <https://doi.org/10.1007/s11998-020-00401-9>.
- [186] G. Gonzalez, A. Chiappone, I. Roppolo, E. Fantino, V. Bertana, F. Perrucci, L. Scaltrito, F. Pirri, M. Sangermano, Development of 3D printable formulations containing CNT with enhanced electrical properties, *Polymer (Guildf).* 109 (2016) 246–253. <https://doi.org/10.1016/j.polymer.2016.12.051>.
- [187] J.S. Manzano, Z.B. Weinstein, A.D. Sadow, I.I. Slowing, Direct 3D Printing of Catalytically Active Structures, *ACS Catal.* 7 (2017) 7567–7577. <https://doi.org/10.1021/acscatal.7b02111>.
- [188] G.A. González Flores, V. Bertana, A. Chiappone, I. Roppolo, L. Scaltrito, S.L. Marasso, M. Cocuzza, G. Massaglia, M. Quaglio, C.F. Pirri, S. Ferrero, Single-Step 3D Printing of Silver-Patterned Polymeric Devices for Bacteria Proliferation Control, *Macromol. Mater. Eng.* 2100596 (2021) 2100596. <https://doi.org/10.1002/mame.202100596>.
- [189] P.F. Costa, H.J. Albers, J.E.A. Linsen, H.H.T. Middelkamp, L. Van Der Hout, R. Passier, A. Van Den Berg, J. Malda, A.D. Van Der Meer, Mimicking arterial thrombosis in a 3D-printed microfluidic: In vitro vascular model based on computed tomography angiography data, *Lab Chip.* 17 (2017) 2785–2792. <https://doi.org/10.1039/c7lc00202e>.
- [190] P. Heo, S. Ramakrishnan, J. Coleman, J.E. Rothman, J.B. Fleury, F. Pincet, Highly Reproducible Physiological Asymmetric Membrane with Freely Diffusing Embedded Proteins in a 3D-Printed Microfluidic Setup, *Small.* 15 (2019) 1–13. <https://doi.org/10.1002/smll.201900725>.
- [191] C.L. Manzanares Palenzuela, M. Pumera, (Bio)Analytical chemistry enabled by 3D printing: Sensors and biosensors, *TrAC - Trends Anal. Chem.* 103 (2018) 110–118. <https://doi.org/10.1016/j.trac.2018.03.016>.
- [192] D.J. Wales, Q. Cao, K. Kastner, E. Karjalainen, G.N. Newton, V. Sans, 3D-Printable Photochromic Molecular Materials for Reversible Information Storage, *Adv. Mater.* 30 (2018) 1–7. <https://doi.org/10.1002/adma.201800159>.
- [193] A.K. Au, W. Lee, A. Folch, Mail-order microfluidics: Evaluation of stereolithography for the production of microfluidic devices, *Lab Chip.* 14 (2014) 1294–1301. <https://doi.org/10.1039/c3lc51360b>.
- [194] A.I. Shallan, P. Smejkal, M. Corban, R.M. Guijt, M.C. Breadmore, Cost-effective three-dimensional printing of visibly transparent microchips within minutes, *Anal. Chem.* 86

(2014) 3124–3130. <https://doi.org/10.1021/ac4041857>.

- [195] H. Gong, M. Beauchamp, S. Perry, A. Woolley, G. Nordin, Optical Approach to Resin Formulation for 3D Printed Microfluidics, *RSC Adv.* 5 (2015) 106621–106632. <https://doi.org/10.1039/C5RA23855B>.
- [196] M.J. Beauchamp, H. Gong, A.T. Woolley, G.P. Nordin, 3D printed microfluidic features using dose control in X, Y, and Z dimensions, *Micromachines.* 9 (2018). <https://doi.org/10.3390/mi9070326>.
- [197] E.K. Parker, A. V. Nielsen, M.J. Beauchamp, H.M. Almughamsi, J.B. Nielsen, M. Sonker, H. Gong, G.P. Nordin, A.T. Woolley, 3D printed microfluidic devices with immunoaffinity monoliths for extraction of preterm birth biomarkers, *Anal. Bioanal. Chem.* 411 (2019) 5405–5413. <https://doi.org/10.1007/s00216-018-1440-9>.
- [198] M.J. Beauchamp, A. V. Nielsen, H. Gong, G.P. Nordin, A.T. Woolley, 3D Printed Microfluidic Devices for Microchip Electrophoresis of Preterm Birth Biomarkers, *Anal. Chem.* 91 (2019) 7418–7425. <https://doi.org/10.1021/acs.analchem.9b01395>.
- [199] C.I. Rogers, K. Qaderi, A.T. Woolley, G.P. Nordin, 3D printed microfluidic devices with integrated valves, *Biomicrofluidics.* 9 (2015) 1–9. <https://doi.org/10.1063/1.4905840>.
- [200] H. Gong, A.T. Woolley, G.P. Nordin, High density 3D printed microfluidic valves, pumps, and multiplexers, *Lab Chip.* 16 (2016) 2450–2458. <https://doi.org/10.1039/c6lc00565a>.
- [201] Y.S. Lee, N. Bhattacharjee, A. Folch, 3D-printed Quake-style microvalves and micropumps, *Lab Chip.* 18 (2018) 1207–1214. <https://doi.org/10.1039/c8lc00001h>.
- [202] S. Takenaga, B. Schneider, E. Erbay, M. Biselli, T. Schnitzler, M.J. Schöning, T. Wagner, Fabrication of biocompatible lab-on-chip devices for biomedical applications by means of a 3D-printing process, *Phys. Status Solidi Appl. Mater. Sci.* 212 (2015) 1347–1352. <https://doi.org/10.1002/pssa.201532053>.
- [203] A.P. Kuo, N. Bhattacharjee, Y.S. Lee, K. Castro, Y.T. Kim, A. Folch, High-Precision Stereolithography of Biomicrofluidic Devices, *Adv. Mater. Technol.* 1800395 (2019) 1–11. <https://doi.org/10.1002/admt.201800395>.
- [204] Z. Wang, N. Martin, D. Hini, B. Mills, K. Kim, Rapid fabrication of multilayer microfluidic devices using the liquid crystal display-based stereolithography 3D printing system, *3D Print. Addit. Manuf.* 4 (2017) 156–164. <https://doi.org/10.1089/3dp.2017.0028>.
- [205] M.J. Männel, L. Selzer, R. Bernhardt, J. Thiele, Optimizing Process Parameters in Commercial Micro-Stereolithography for Forming Emulsions and Polymer Microparticles in Nonplanar Microfluidic Devices, *Adv. Mater. Technol.* 4 (2019) 1–10. <https://doi.org/10.1002/admt.201800408>.
- [206] F. Kotz, P. Risch, D. Helmer, B.E. Rapp, Highly fluorinated methacrylates for optical 3D printing of microfluidic devices, *Micromachines.* 9 (2018). <https://doi.org/10.3390/mi9030115>.
- [207] C. Yeung, S. Chen, B. King, H. Lin, K. King, F. Akhtar, G. Diaz, B. Wang, J. Zhu, W. Sun, A. Khademhosseini, S. Emaminejad, A 3D-printed microfluidic-enabled hollow microneedle architecture for transdermal drug delivery, *Biomicrofluidics.* 13 (2019). <https://doi.org/10.1063/1.5127778>.
- [208] N. Bhattacharjee, C. Parra-Cabrera, Y.T. Kim, A.P. Kuo, A. Folch, Desktop-Stereolithography 3D-Printing of a Poly(dimethylsiloxane)-Based Material with Sylgard-184 Properties, *Adv. Mater.* 30 (2018) 1–7. <https://doi.org/10.1002/adma.201800001>.
- [209] S. Zips, L. Hiendlmeier, L.J.K. Weiß, H. Url, T.F. Teshima, R. Schmid, M. Eblenkamp, P. Mela, B. Wolfrum, Biocompatible, Flexible, and Oxygen-Permeable Silicone-Hydrogel Material for Stereolithographic Printing of Microfluidic Lab-On-A-Chip and Cell-Culture Devices, *ACS*

- Appl. Polym. Mater. (2020). <https://doi.org/10.1021/acsapm.0c01071>.
- [210] G. Gonzalez, A. Chiappone, K. Dietliker, C.F. Pirri, I. Roppolo, Fabrication and Functionalization of 3D Printed Polydimethylsiloxane-Based Microfluidic Devices Obtained through Digital Light Processing, *Adv. Mater. Technol.* 5 (2020) 2000374. <https://doi.org/10.1002/admt.202000374>.
- [211] J. Berger, M.Y. Aydin, R. Stavins, J. Heredia, A. Mostafa, A. Ganguli, E. Valera, R. Bashir, W.P. King, Portable Pathogen Diagnostics Using Microfluidic Cartridges Made from Continuous Liquid Interface Production Additive Manufacturing, *Anal. Chem.* 93 (2021) 10048–10055. <https://doi.org/10.1021/acs.analchem.1c00654>.
- [212] Carbon3D, RPU 70, (2021). <https://www.carbon3d.com/materials/rpu-70/> (accessed August 21, 2021).
- [213] W. Wu, A. Deconinck, J.A. Lewis, Omnidirectional printing of 3D microvascular networks, *Adv. Mater.* 23 (2011) 178–183. <https://doi.org/10.1002/adma.201004625>.
- [214] K.S. Lim, J.H. Galarraga, X. Cui, G.C.J. Lindberg, J.A. Burdick, T.B.F. Woodfield, Fundamentals and Applications of Photo-Cross-Linking in Bioprinting, *Chem. Rev.* (2020). <https://doi.org/10.1021/acs.chemrev.9b00812>.
- [215] J.Y. Lee, J. An, C.K. Chua, Fundamentals and applications of 3D printing for novel materials, *Appl. Mater. Today.* 7 (2017) 120–133. <https://doi.org/10.1016/j.apmt.2017.02.004>.
- [216] M. Layani, X. Wang, S. Magdassi, Novel Materials for 3D Printing by Photopolymerization, *Adv. Mater.* 30 (2018) 1–7. <https://doi.org/10.1002/adma.201706344>.
- [217] L.S. Andrews, J.J. Clary, Review of the toxicity of multifunctional acrylates, *J. Toxicol. Environ. Health.* (1986). <https://doi.org/10.1080/15287398609530916>.
- [218] F. Zhu, J. Skommer, T. Friedrich, J. Kaslin, D. Wlodkowic, 3D printed polymers toxicity profiling: A caution for biodevice applications, in: *SPIE Micro+Nano Mater. Devices*, Appl. Symp., Sidney, Australia, n.d. <https://doi.org/10.1117/12.2202392>.
- [219] R. Zhang, N.B. Larsen, Stereolithographic hydrogel printing of 3D culture chips with biofunctionalized complex 3D perfusion networks, *Lab Chip.* 17 (2017) 4273–4282. <https://doi.org/10.1039/c7lc00926g>.
- [220] A.D. Benjamin, R. Abbasi, M. Owens, R.J. Olsen, D.J. Walsh, T.B. Lefevre, J.N. Wilking, Light-based 3D printing of hydrogels with high-resolution channels, *Biomed. Phys. Eng. Express.* (2019). <https://doi.org/10.1088/2057-1976/aad667>.
- [221] A.A. Pawar, G. Saada, I. Cooperstein, L. Larush, J.A. Jackman, S.R. Tabaei, N.J. Cho, S. Magdassi, High-performance 3D printing of hydrogels by water-dispersible photoinitiator nanoparticles, *Sci. Adv.* 2 (2016). <https://doi.org/10.1126/sciadv.1501381>.
- [222] Y. Zhang, D. An, Y. Pardo, A. Chiu, W. Song, Q. Liu, F. Zhou, S.P. McDonough, M. Ma, High-water-content and resilient PEG-containing hydrogels with low fibrotic response, *Acta Biomater.* 53 (2017) 100–108. <https://doi.org/10.1016/j.actbio.2017.02.028>.
- [223] Y.S. Kim, K. Cho, H.J. Lee, S. Chang, H. Lee, J.H. Kim, W.G. Koh, Highly conductive and hydrated PEG-based hydrogels for the potential application of a tissue engineering scaffold, *React. Funct. Polym.* 109 (2016) 15–22. <https://doi.org/10.1016/j.reactfunctpolym.2016.09.003>.
- [224] C.M. González-Henríquez, F.E. Rodríguez-Umanzor, J. Almagro-Correa, M.A. Sarabia-Vallejos, E. Martínez-Campos, M. Esteban-Lucía, A. del Campo-García, J. Rodríguez-Hernández, Biocompatible fluorinated wrinkled hydrogel films with antimicrobial activity, *Mater. Sci. Eng. C.* 114 (2020) 111031. <https://doi.org/10.1016/j.msec.2020.111031>.
- [225] M.J. Männel, C. Fischer, J. Thiele, A Non-Cytotoxic Resin for Micro-Stereolithography for Cell Cultures of HUVECs, *Micromachines.* 11 (2020). <https://doi.org/10.3390/mi11030246>.

- [226] C. Warr, J.C. Valdoz, B.P. Bickham, C.J. Knight, N.A. Franks, N. Chartrand, P.M. Van Ry, K.A. Christensen, G.P. Nordin, A.D. Cook, Biocompatible PEGDA Resin for 3D Printing, *ACS Appl. Bio Mater.* 3 (2020) 2239–2244. <https://doi.org/10.1021/acsabm.0c00055>.
- [227] MicronInc, FDA Approved 3D Printer Resins, (2017). <https://www.micron dental.com/regulatory/fda-approved-cleared-3d-printer-resins> (accessed October 30, 2019).
- [228] K. Piironen, M. Haapala, V. Talman, P. Järvinen, T. Sikanen, Cell adhesion and proliferation on common 3D printing materials used in stereolithography of microfluidic devices, *Lab Chip.* 20 (2020) 2372–2382. <https://doi.org/10.1039/d0lc00114g>.
- [229] S. Krefß, R. Schaller-Ammann, J. Feiel, J. Priedl, C. Kasper, D. Egger, 3D printing of cell culture devices: Assessment and prevention of the cytotoxicity of photopolymers for stereolithography, *Materials (Basel).* 13 (2020). <https://doi.org/10.3390/ma13133011>.
- [230] R.P. Rimington, A.J. Capel, D.J. Player, R.J. Bibb, S.D.R. Christie, M.P. Lewis, Feasibility and Biocompatibility of 3D-Printed Photopolymerized and Laser Sintered Polymers for Neuronal , Myogenic , and Hepatic Cell Types, *Macromol. Biosci.* 1800113 (2018) 1–12. <https://doi.org/10.1002/mabi.201800113>.
- [231] M. Schuster, C. Turecek, B. Kaiser, J. Stampfl, R. Liska, F. Varga, Evaluation of biocompatible photopolymers I: Photoreactivity and mechanical properties of reactive diluents, *J. Macromol. Sci. Part A Pure Appl. Chem.* 44 (2007) 547–557. <https://doi.org/10.1080/10601320701235958>.
- [232] Y. Zhang, Post-3D printing modification for improved biomedical applications, *Int. J. Bioprinting.* 3 (2017). <https://doi.org/10.18063/ijb.2017.02.001>.
- [233] G. Gonzalez, D. Baruffaldi, C. Martinengo, A. Angelini, A. Chiappone, I. Roppolo, F.C. Pirri, F. Frascella, Materials Testing for the Development of Biocompatible Devices through Vat-Polymerization 3D Printing, *Nanomaterials.* 10 (2020) 1788. <https://doi.org/10.3390/nano10091788>.
- [234] X. Wang, X. Cai, Q. Guo, T. Zhang, B. Kobe, J. Yang, I3DP, a robust 3D printing approach enabling genetic post-printing surface modification, *Chem. Commun.* 49 (2013) 10064–10066. <https://doi.org/10.1039/c3cc45817b>.
- [235] A. Chiadò, G. Palmara, A. Chiappone, C. Tanzanu, C.F. Pirri, I. Roppolo, F. Frascella, A modular 3D printed lab-on-a-chip for early cancer detection, *Lab Chip.* 20 (2020) 665–674. <https://doi.org/10.1039/c9lc01108k>.
- [236] J.A. Calvo-Haro, J. Pascau, J.M. Asencio-Pascual, F. Calvo-Manuel, M.J. Cancho-Gil, J.F. Del Cañizo López, M. Fanjul-Gómez, R. García-Leal, G. González-Casaurreán, M. González-Leyte, J.A. León-Luis, L. Mediavilla-Santos, S. Ochandiano-Caicoya, R. Pérez-Caballero, A. Ribed-Sánchez, J. Río-Gómez, E. Sánchez-Pérez, J. Serrano-Andreu, M. Tousidonis-Rial, J. Vaquero-Martín, S. García San José, R. Perez-Mañanes, Point-of-care manufacturing: a single university hospital's initial experience, *3D Print. Med.* 7 (2021) 1–14. <https://doi.org/10.1186/s41205-021-00101-z>.
- [237] H.N. Chan, M.J.A. Tan, H. Wu, Point-of-care testing: Applications of 3D printing, *Lab Chip.* 17 (2017) 2713–2739. <https://doi.org/10.1039/c7lc00397h>.
- [238] D. Wang, H.N. Chan, Z. Liu, S. Micheal, L. Li, D.B. Baniani, M.J.A. Tan, L. Huang, J. Wang, H. Wu, Recent Developments in Microfluidic -Based Point-of-care Testing (POCT) Diagnoses, 2020. <https://doi.org/10.1002/9783527818341.ch8>.
- [239] C. Tzivelekis, P. Sgardelis, K. Waldron, R. Whalley, D. Huo, K. Dalgarno, Fabrication routes via projection stereolithography for 3D-printing of microfluidic geometries for nucleic acid amplification, *PLoS One.* 15 (2020) 1–21. <https://doi.org/10.1371/journal.pone.0240237>.

- [240] K. Kadimisetty, J. Song, A.M. Doto, Y. Hwang, J. Peng, M.G. Mauk, F.D. Bushman, R. Gross, J.N. Jarvis, C. Liu, Fully 3D printed integrated reactor array for point-of-care molecular diagnostics, *Biosens. Bioelectron.* 109 (2018) 156–163. <https://doi.org/10.1016/j.bios.2018.03.009>.
- [241] X. Wang, M. Jiang, Z. Zhou, J. Gou, D. Hui, 3D printing of polymer matrix composites: A review and prospective, *Compos. Part B Eng.* 110 (2017) 442–458. <https://doi.org/10.1016/j.compositesb.2016.11.034>.
- [242] Ultimaker, Ultimaker S3: Powerful, professional 3D printing, (n.d.). <https://ultimaker.com/3d-printers/ultimaker-s3> (accessed August 16, 2021).
- [243] BMF Materials Inc., Industrial Micro-Precision 3D Printers, (2020). <https://bmf3d.com/>.
- [244] Q. Ge, Z. Li, Z. Wang, K. Kowsari, W. Zhang, X. He, J. Zhou, N.X. Fang, Projection micro stereolithography based 3D printing and its applications, *Int. J. Extrem. Manuf.* 2 (2020). <https://doi.org/10.1088/2631-7990/ab8d9a>.
- [245] N.F. Ayub, S. Hashim, J. Jamaluddin, N. Adrus, New UV LED curing approach for polyacrylamide and poly(: N -isopropylacrylamide) hydrogels, *New J. Chem.* (2017). <https://doi.org/10.1039/c7nj00176b>.
- [246] V. Mucci, C. Vallo, Efficiency of 2,2-dimethoxy-2-phenylacetophenone for the photopolymerization of methacrylate monomers in thick sections, *J. Appl. Polym. Sci.* (2012). <https://doi.org/10.1002/app.34473>.
- [247] B. Steyrer, P. Neubauer, R. Liska, J. Stampfl, Visible light photoinitiator for 3D-printing of tough methacrylate resins, *Materials (Basel)*. 10 (2017) 1–11. <https://doi.org/10.3390/ma10121445>.
- [248] H.K. Park, M. Shin, B. Kim, J.W. Park, H. Lee, A visible light-curable yet visible wavelength-transparent resin for stereolithography 3D printing, *NPG Asia Mater.* 10 (2018) 82–89. <https://doi.org/10.1038/s41427-018-0021-x>.
- [249] B.D. Fairbanks, M.P. Schwartz, C.N. Bowman, K.S. Anseth, Photoinitiated polymerization of PEG-diacrylate with lithium phenyl-2,4,6-trimethylbenzoylphosphinate: polymerization rate and cytocompatibility, *Biomaterials*. 30 (2009) 6702–6707. <https://doi.org/10.1016/j.biomaterials.2009.08.055>.
- [250] K. Wang, K. Yang, Q. Yu, Novel polymeric photoinitiators with side-chain benzophenone: Facile synthesis and photopolymerization properties without coinitiator, *Prog. Org. Coatings*. (2014). <https://doi.org/10.1016/j.porgcoat.2014.06.026>.
- [251] H. Matsushima, S. Hait, Q. Li, H. Zhou, M. Shirai, C.E. Hoyle, Non-extractable photoinitiators based on thiol-functionalized benzophenones and thioxanthenes, *Eur. Polym. J.* (2010). <https://doi.org/10.1016/j.eurpolymj.2010.03.003>.
- [252] Y.C. Chen, J.L. Ferracane, S.A. Prahl, Quantum yield of conversion of the photoinitiator camphorquinone, *Dent. Mater.* (2007). <https://doi.org/10.1016/j.dental.2006.06.005>.